To the Graduate Council:

I am submitting herewith a dissertation written by George Larry Copeland entitled "An Investigation of Alloying Effects in Aluminum Dispersion Strengthened with Al_2O_3." I recommend that it be accepted in partial fulfillment of the requirements for the degree of Doctor of Philosophy, with a major in Metallurgical Engineering.

J. E. Spruiell

J. E. Spruiell, Major Professor

We have read this dissertation
and recommend its acceptance:

Carl J. Montrone

Ben T. Alexi

V. R. R. Uppaluri

E. E. Stansbury

Accepted for the Council:

Hilton A. Smith

Vice Chancellor
Graduate Studies and Research

AN INVESTIGATION OF ALLOYING EFFECTS IN ALUMINUM DISPERSION STRENGTHENED WITH Al_2O_3

A Dissertation

Presented for the

Doctor of Philosophy

Degree

The University of Tennessee

George Larry Copeland

March 1975

ACKNOWLEDGMENTS

The research for this dissertation was performed at the Oak Ridge National Laboratory operated by Union Carbide Corporation under contract to the United States Atomic Energy Commission. The author wishes to express his appreciation to the many members of the Oak Ridge National Laboratory staff who contributed to this work. The author especially thanks his major professor, Dr. J. E. Spruiell, for his advice, encouragement, and patience.

1214590

ABSTRACT

The purpose of this investigation was to determine the effects of alloying elements on the mechanical properties of aluminum dispersion strengthened by its own oxide, commonly referred to as sintered aluminum product (SAP). SAP is noted for its high strength at elevated temperatures compared to conventional aluminum alloys. However, it has seen little application due to its low ductility at high temperatures and its relatively low strength at room temperature compared to conventional aluminum alloys. Two types of alloying elements were investigated to determine if the room-temperature strength could be improved and if, through lowering the oxide content, the high-temperature ductility could be improved. Magnesium was investigated for its solid solution strengthening in one type alloy. The other type alloy involved further dispersion strengthening through adding the elements iron, molybdenum, zirconium, chromium, vanadium, and titanium which form highly stable intermetallic compounds with aluminum.

To evaluate the effects of the alloying, fabrication techniques were developed which produced uniform and reproducible rods for testing. Prealloyed powders were produced by atomizing the molten alloys and collecting the powders in water. This procedure produced uniform powders with a very fine distribution of the intermetallic compounds. Fabrication into rods then included ball-milling, vacuum hot pressing, vacuum heat treating, and hot extrusion.

The magnesium additions improved strengths up to 200°C with little effect above that temperature. Room-temperature tensile strengths up to 77,000 psi were obtained which are comparable to the strengths

obtained in conventional aluminum alloys. The additional dispersion strengthening of the intermetallic compounds is additive to that of the oxide from room temperature to 450°C. No significant improvements in ductility are obtained by reducing the oxide content since even at very low ball-milling times (i.e., low oxide contents) the uniform elongation at 450°C is typically 0.5%. Good combinations of strength and ductility at 450°C were obtained in some of the alloys containing intermetallic compounds with no ball-milling. Typical properties at this temperature were tensile strengths of 7,000 psi, uniform elongation of 3%, and total elongation of 35%.

TABLE OF CONTENTS

CHAPTER		PAGE
I.	INTRODUCTION	1
II.	BACKGROUND AND LITERATURE REVIEW	3
	Strengthening Mechanisms	3
	Solid solution strengthening	3
	Work hardening	4
	Precipitation strengthening	5
	Dispersion strengthening	6
	Fracture Mechanisms	10
	Properties of Commercially Available SAP	11
	Alloying Effects in Aluminum	14
	Magnesium	14
	Iron	15
	Molybdenum	16
	Zirconium	16
	Titanium	16
	Vanadium	17
	Chromium	17
	Previous Work on Alloying of Aluminum–Aluminum Oxide Dispersions	18
III.	DEVELOPMENT OF FABRICATION PARAMETERS	21
	Dispersion Preparation	21
	Selection of preparation technique	22
	Determination of ball-milling conditions	22

CHAPTER		PAGE
	Consolidation	27
	Stabilization of oxide	27
	Initial processing studies	30
	Process scale-up	32
	Effect of Impurities	39
	Hydrogen	39
	Iron	41
	Carbon	42
	Process Evaluation	43
IV.	PRODUCTION OF ALLOYS	49
	Powder Production and Characterization	49
	Production of Alloy Rods	51
V.	EVALUATION PROCEDURES	54
	Tensile Testing	54
	Oxide Content Determination	55
	Transmission Electron Microscopy	57
	Optical Metallography	57
VI.	RESULTS	58
VII.	DISCUSSION OF FRACTURE MECHANISM	70
VIII.	DISCUSSION OF STRENGTHENING MECHANISMS	87
IX.	CONCLUSIONS	89
LIST OF REFERENCES		91
APPENDIX		95
VITA		105

LIST OF TABLES

TABLE		PAGE
1.	Characteristics of the Methods of Dispersion Preparation	23
2.	Billet Consolidation Processes	30
3.	Effect of Billet Consolidation Process on Oxide Content and Tensile Strength of Extruded Rod	32
4.	Strength of SAP Rods Extruded from Billets of Various Densities	34
5.	Effect of Consolidation Route on Experimental SAP Rods	36
6.	Effect of Billet Vacuum Anneal Duration on Thermal Stability of Process B Extrusions	38
7.	Effect of Hydrogen on the Mechanical Properties of Extruded SAP Materials	40
8.	Effect of Iron on Mechanical Properties of Extruded Rods	42
9.	Effect of Carbon on Mechanical Properties of Extruded Rods	44
10.	Composition and Strength of Rods from Reproducibility Study ...	45
11.	Screen Analyses of Atomized Powders	50
12.	Chemical Content of Atomized Powders	51
13.	Tensile Properties of Dispersion Strengthened Unalloyed Aluminum	96
14.	Tensile Properties of Dispersion Strengthened Aluminum-2.0% Magnesium Alloys	97
15.	Tensile Properties of Dispersion Strengthened Aluminum-4.3% Magnesium Alloys	98
16.	Tensile Properties of Dispersion Strengthened Aluminum-6.2% Magnesium Alloys	100

TABLE PAGE

17. Tensile Properties of Dispersion Strengthened Alloy CA-0218 100

18. Tensile Properties of Dispersion Strengthened Alloy CA-0219 101

19. Tensile Properties of Dispersion Strengthened Alloy CA-0222 102

20. Tensile Properties of Dispersion Strengthened Alloy CA-0223 103

21. Tensile Properties of Dispersion Strengthened Alloy CA-0224 104

LIST OF FIGURES

FIGURE		PAGE
1.	Tensile Strength and Ductility of XAP-001	13
2.	The Effect of Milling Time on Oxide Content of −100 Mesh Aluminum Powder	25
3.	Effect of Mill Diameter on Oxide Content for Constant Milling Conditions	26
4.	Effect of Temperature on Degassing Ball-Milled Aluminum Powder	28
5.	Strength and Uniform Elongation of Experimental SAP and Commercial SAP 895 as a Function of Testing Temperature	46
6.	Comparison of Longitudinal Microstructure (100X) of Experimental SAP (right) and SAP 895 (left)	47
7.	Comparison of Transmission Electron Microstructure (25,000X) of Experimental SAP (top) and SAP 895 (bottom)	48
8.	Outline of Procedure for Production of Experimental Dispersion Strengthened Aluminum Alloys	52
9.	Tensile Specimen	54
10.	Pull Rod Setup for Elevated Temperature Tensile Testing of SAP	56
11.	Room-Temperature Tensile Properties of Representative Experimental Alloys as a Function of Ball-Milling Time	59
12.	Tensile Properties at 450°C of Representative Experimental Alloys as a Function of Ball-Milling Time	60
13.	Tensile Strength of Experimental Magnesium Alloys with No Ball Milling	61

FIGURE PAGE

14. Uniform Elongation of Experimental Magnesium Alloys with No Ball-Milling 62

15. Tensile Strength of Experimental Magnesium Alloys with 2 Hours Ball-Milling 63

16. Uniform Elongation of Experimental Magnesium Alloys with 2 Hours Ball-Milling 64

17. Tensile Properties of Experimental Alloyed and Unalloyed SAP as a Function of Testing Temperature 66

18. Tensile Properties of Experimental Alloys with No Ball-Milling as a Function of Testing Temperature 67

19. Tensile Properties of Experimental Alloys with 10 Hours Ball-Milling and a Commercial Alloy as a Function of Testing Temperature 69

20. Scanning Electron Micrographs of Fracture Surface of Experimental Unalloyed SAP with 2 Hours Ball-Milling 71

21. Scanning Electron Micrographs of Fracture Surface of Alloy M-6 with 2 Hours Ball-Milling 72

22. Scanning Electron Micrographs of Fracture Surface of Alloy CA-0223 with 2 Hours Ball-Milling 73

23. Scanning Electron Micrographs of Fracture Surface of Alloy M-6 with 10 Hours Ball-Milling 74

24. Scanning Electron Micrographs of Fracture Surface of Experimental Unalloyed SAP with 8 Hours Ball-Milling 75

25. Scanning Electron Micrographs of Fracture Surface of Alloy CA-0223 with 10 Hours Ball-Milling 76

FIGURE PAGE

26. Typical Features Observed After Fracture of Unalloyed SAP at High Temperature 77

27. Tensile Strength of Unalloyed SAP at −196°C as a Function of Prior Prestrain at 450°C 79

28. Tensile Strength of Unalloyed SAP at −196°C as a Function of the Amount of Cross-Sectional Area Lost Due to Voiding During Prestrain 79

29. Transmission Electron Micrograph of Alloy CA-0223 with No Ball-Milling 81

30. Transmission Electron Micrograph of Alloy CA-0223 with 2 Hours Ball-Milling 82

31. Transmission Electron Micrograph of Alloy CA-0223 with 8 Hours Ball-Milling 83

32. Transmission Electron Micrograph of Alloy CA-0223 with 10 Hours Ball-Milling (50,000X) 84

33. Transmission Electron Micrograph of Alloy CA-0223 with 10 Hours Ball-Milling (100,000X) 85

CHAPTER I

INTRODUCTION

Aluminum dispersion strengthened by its own oxide was developed by Irman (1) over 20 years ago and is noted for its excellent elevated temperature creep and tensile strength. The material (usually referred to as "sintered aluminum product" or SAP) is generally produced by ball-milling aluminum powder to increase its oxide content and then consolidating the powder by hot pressing and hot extruding. The high strength at elevated temperature combined with good corrosion resistance and good nuclear properties led to the selection of SAP as the cladding material for organic-cooled, heavy-water-moderated nuclear reactors such as the Heavy Water Organic Cooled Reactor (HWOCR) (2) in the United States and the Orgel (3) in Europe. Although these reactors were never fully developed, the interest in them resulted in much study and development work on SAP-type materials. The result was higher purity, more uniform, and reproducible SAP-type materials. (4,5) In spite of these improvements, there has been virtually no commercial use of SAP-type materials. Two drawbacks of SAP which have possibly contributed to this lack of use are (1) the very low uniform elongation in tension at elevated temperatures, and (2) the relatively low tensile strength at room temperature compared to the stronger conventional aluminum alloys.

The objectives of this work were to determine if, through alloying, the room-temperature strength of SAP could be improved without sacrificing high-temperature properties, and if higher strength could allow lower oxide contents for improved elongation at high temperature. Two promising

alloy types are solid solution strengthening and further dispersion strengthening with slightly soluble intermetallic compounds. Magnesium is the obvious choice for solid solution additions due to its high solid solubility and effective solid solution strengthening. Towner (6) has shown that powdered alloys containing finely distributed intermetallic compounds can be produced by atomizing aluminum alloys containing the elements, iron, molybdenum, zirconium, titanium, tungsten, and other low solid solubility elements which form very stable compounds with aluminum. Alloys produced by consolidating these powders by hot pressing and extruding were found to have improved strength at high temperatures and to be stable at temperatures up to 400°C. (6)

To determine the effects of these alloying additions on the tensile properties of dispersion-strengthened aluminum, the following alloys were produced and tensile tested at temperatures from 27 to 450°C:

1. aluminum-magnesium alloys containing 2 to 6% magnesium and oxide contents of 0.5% as-atomized up to 10% after ball-milling for 12 hours, and
2. aluminum alloys containing various additions of molybdenum, iron, zirconium, chromium, vanadium, and titanium both as-atomized and after ball-milling up to 12 hours.

To evaluate the effects of these alloying elements, it was first necessary to develop fabrication techniques which resulted in uniform and reproducible rods for testing.

CHAPTER II

BACKGROUND AND LITERATURE REVIEW

Strengthening Mechanisms

Metal crystals should have strengths of the order 10^6 psi based on the atomic attraction forces. Strengths approaching this level are observed in some very small nearly perfect crystals or "whiskers." However, metals generally exhibit strengths much lower than this due to imperfections called dislocations which can be forced to move through crystals at much lower stresses, resulting in net plastic flow. The generation, movement, and interactions of dislocations are well understood and are discussed at length in most texts on physical metallurgy. (7,8) Most of the methods of strengthening metals are based on impeding the movement of the dislocations. The commercially important aluminum alloys are strengthened almost exclusively either by cold working or by precipitation strengthening. Solid solution strengthening plays an important role in aluminum-magnesium alloys for special applications. Dispersion strengthening is very effective in aluminum (SAP) but has seen very little application for reasons discussed previously.

Solid Solution Strengthening

An alloying element going into solid solution always strengthens the solvent metal. (7) In dilute solutions the amount of strengthening is generally proportional to the solute concentrations, and if more than one solute is present their effects are usually additive. The strengthening produced by a given element is dependent on the difference

in size between the solute and the solvent and on their differences in electronic structure. It appears that dislocation movements are not greatly hindered by a random array of solute atoms on the solvent lattice. However, if the solute atoms tend to collect preferentially at the dislocations, the force required to move them may be increased considerably. The reason for solute atoms collecting on dislocations is that the total energy of the system is often lowered if the stress fields created by the solute atoms are combined with those of the dislocation. When this occurs the dislocation is said to be locked by a solute atmosphere. Other interactions which may impede dislocation movement are preferential segregation of solute atoms in stacking faults or in ordered arrays. This strengthening mechanism becomes less effective at higher temperatures where diffusion becomes more rapid.

Work Hardening

Deformation of metals occurs primarily by the motion of existing dislocations and by the creation of new dislocations through mechanisms such as the Frank-Read source. (7) This dislocation glide occurs on intersecting slip planes within the grain and with mutual interference with slip planes from adjacent grains. The interactions of dislocations cause further deformation to become more difficult thus strengthening the metal through strain hardening or work hardening. Depending on whether the dislocations that cut across one another are of the edge or screw type, the result may be the creation of a line of vacancies or interstilials in the lattice. Part of a dislocation may be forced into a parallel slip plan with the discontinuity between the two portions called a "jog." The addition of a soluble alloying element may either increase or decrease the rate of strain hardening.

A part of the energy expended in deformation is stored in the deformed metal structure. This stored energy acts as a thermodynamic driving force which tends to return the metal to its undeformed state if the temperature is raised sufficiently for the required reactions to occur at an appreciable rate. Thus, as the temperature is raised the processes of recovery and recrystallization return the metal to the fully annealed state. Therefore, work hardening is a suitable strengthening mechanism only for service conditions where the metal will never be heated to the point that softening will occur to an extent that will lower the strength below the design level.

Precipitation Strengthening

The necessary condition for precipitation from solid solution is the existence of a sloping solvus line, that is, decreasing solid solubility with decreasing temperature. (7) The precipitate is usually a compound of the solute and solvent metal. The steps involved in accomplishing the strengthening include: (1) solution heat treating the metal at a high temperature to dissolve a maximum amount of the second phase, (2) cooling quickly to retain the second phase in a supersaturated solid solution, and (3) precipitation treatment allowing the second phase to precipitate from solid solution under conditions such that a desirable distribution of second phase is obtained.

The strength obtained from precipitate particles depends primarily on their distribution, that is, the distance separating them. The basic mechanism of strengthening is the same as for dispersion strengthening which will be discussed below. Important differences exist though, especially at the initial precipitation and as the precipitate approaches

equilibrium. In the early stages of precipitation, a transition lattice is formed which is coherent with the parent lattice. This transition precipitate is especially effective in strengthening since the strain it exerts on the lattice lowers the effective particle separation. As aging progresses, the particles lose coherency with the lattice and continue to grow in size thus increasing particle separation. Eventually, if given sufficient time at temperature, the particles become too large for effective strengthening and the material is said to be overaged. Thus, like work hardening, precipitation strengthening is effective only under conditions where the material will not be exposed to excessive temperatures. Some alloys even become overaged with time at room temperature.

Dispersion Strengthening

A dispersion strengthened alloy is one in which a discontinuous minority phase is randomly dispersed in a matrix, thereby strengthening the alloy. The high-temperature limit of usefulness of the alloy is determined by the temperature at which the dispersion becomes unstable by either dissolving in the matrix or by agglomerating and increasing the particle separation distance enough that no effective strengthening is obtained. The stability of the dispersion is determined by its thermodynamic free energy of formation, the solubilities and diffusivities of the components, and the initial distribution of the dispersed phase.

Several surveys have been published covering the extensive literature on dispersion strengthening, so only the highlights of the most important theories on the yield stress will be repeated here. Bunshah and Goetzel (9) have published a very thorough review of the literature up

through 1959 which includes fabrication techniques, strengthening mechanisms, and an anotated bibliography. More recently, Ansell (10) has critically compared the various strengthening mechanisms for dispersions.

1. Direct Particle-Dislocation Interactions. - (a) Dislocation bowing. Orowan (11) proposed a dislocation model to predict the strength of dispersions based on the bowing of a dislocation as it passes two particles blocking its progress on a slip plane. The dislocation first bows between the particles, then pinches off leaving a loop around the particles as the dislocation passes on. The buildup of loops around the particles provides further resistance to the passage of dislocations. This process appears to be valid if the dislocations are confined to motion in the slip plane, and if the build up of stress around the particle does not shear or fracture the particle.

(b) Cross slip. Ashby (12) modified the Orowan theory by proposing that dislocations can bypass particles by a double cross slip mechanism. An edge dislocation moves along the slip plane until it encounters two particles and begins Orowan bowing between them. During bowing screw components of the dislocation form. Due to short-range interaction stresses the screw components cross slip out of the plane. The screw components of opposite sign are attached to each other and annihilate leaving a prismatic dislocation loop around the particle and a corresponding prismatic jog in the dislocation line. Dislocations of this configuration are frequently observed in deformed two-phase alloys.

(c) Particle shear. Kelly and Nicholson (13) and Ansell and Lenel (14) have proposed models to account for the yield strength of dispersion-strengthened alloys when particle shear controls the yield strength. Kelly and Nicholson (13) limit their model to coherent dispersed particles and calculate the yield strength based on balancing the energy required to move the dislocation segment with the energy required for the particle to shear. The energy increments associated with the following structural changes as the particle shears are summed: (1) an increase in particle-matrix interface area, (2) antiphase boundary formation, and (3) dipole extension. Ansell and Lenel (14) argue that particle shear will result from the shear stress built up by piled-up dislocations around or against the particles. They extend the treatment to randomly oriented noncoherent particles which will shear due to dislocation generation within the particle. Ansell (10) further argues that at high strains, the deformation modes in both phases could not satisfy strain compatibility, leading to failure of the particle-matrix interface and void formation.

2. Indirect Particle-Dislocation Effects. – (a) Coherent misfit strain. In a coherent particle the lattice periodicity, spacing, and orientation closely match those of the matrix. Any deviation in this lattice match is usually accommodated by a combination of lattice strains and a defect structure in the interface. Mott and Nabarro (15) proposed a dislocation model to account for the effect of coherent particles on the strength of two-phase alloys based on the interactions of the dislocations with the strain fields around particles because of misfit.

This effect is relatively minor compared to the direct interactions of dislocations with dispersed particles.

(b) Thermally induced substructure. In two-phase alloys where the difference in thermal expansion coefficients of the matrix and particle are large, dislocations may be generated in the matrix adjacent to each particle to relieve thermally induced stresses. Dew-Hughes (16) proposed that the yield strength of these alloys could be controlled by the interaction of matrix slip dislocations with the thermally induced dislocation substructure. Although this mechanism probably contributes to the strength, the magnitude is likely to be small compared to direct interactions with the particles.

(c) Processing induced substructure. In order to fabricate dispersion strengthened alloys from metal and oxide powders extensive hot processing is usually utilized. Several investigators have attempted to relate this processing to a deformation-induced substructure which controls the yield strength of these alloys. Grant and Preston (17,18) linked the strength of several types of alloys to their processing history. They proposed that the strength was derived from stored energy of deformation from the high strain rate hot processing. They suggested that the stored energy is retained by a defect structure resulting from pinning of dislocation arrays and low-angle boundaries by the dispersed oxide phase.

Guyot (19) and others proposed that the dispersed phase induces forest dislocation generation during processing and stabilizes the forest structure once it is formed. Frazer et al. (20) empirically linked the yield stress of thoria-nickel powder products with a substructure induced

during hot processing. They postulated that the main factors contributing to the strength are a fibrous texture and a substructure consisting of subgrain boundaries and dislocation tangles anchored by the dispersed phase particles. Processing technique certainly influences the strength of two phase alloys insofar as it determines the distribution of the second phase. However, there is substantial evidence that retained substructure is not the strength controlling factor since complete recrystallization does not significantly lower the strength of dispersion-strengthened alloys.

Fracture Mechanisms

The fracture path in metals is either transgranular or intergranular. A mixture of the two may occur on the fracture surface. Transgranular fracture generally takes place by cleavage or corrosion along crystallographic planes, by formation and coalescence of microvoids, or by the slow progression of a fatigue crack. Intergranular fracture may be either a perfect separation of the grains at the grain boundaries or the plastic formation of voids along the grain boundaries. The fracture surfaces exhibit markings and topography characteristic of the mechanisms of fracture operating at both initiation and propagation of fracture. These markings can often be differentiated by transmission electron microscopy of replicas of the surface or direct observation of the fracture topography by scanning electron microscopy.

Harman and Nolan (21,22) have studied the fracture of dispersion-strengthened aluminum using both replicas and scanning electron microscopy. The elevated-temperature tensile testing of dispersion-strengthened

aluminum generally is characterized by three modes of fracture – separation, tearing, and shear, each of which is associated with ductile fracture. Fracture initiates as separation, which occurs as voids form and grow and coalesce at sites throughout the material. The oxide particles and agglomerates provide excellent sites for the voiding and separation process. This separation leads to stress concentrations and uneven loading in adjacent areas which results in the tearing fracture mode. The fracture advances from one void to the next by a tearing action with considerable local deformation. As fracture proceeds and the load is concentrated on a smaller cross section, final failure usually occurs by shearing at a relatively high rate due to the high local stress level. The relative area of fracture surface exhibiting each of these fracture modes is influenced markedly by test temperature and strain rate.

Properties of Commercially Available SAP

The commercially produced SAP in the early 1960's was not of adequate quality for nuclear applications because of structural instability at 400 and 500°C, inhomogeneity in oxide dispersion, and presence of large inclusions of iron containing particles. (23) The structural instability at high temperature is due to release of internal hydrogen causing blisters and internal cracks. Harman (24) reviewed the literature and compiled the available strength and elongation data for a particular SAP alloy, Alcoa's XAP-001. This revealed a relatively large scatterband of these mechanical properties when plotted versus testing temperatures. However, when Harman compared his own test results under carefully controlled

strain rates and temperatures, he observed that the different testing rates alone could account for most of the scatterband. This is shown in Figure 1 from Harman's report. (24) Thus, differences in strain rates which were often not reported or controlled accounts for much of the variability in reported mechanical properties in SAP products.

Shortly before the present research began, Euratom workers (23) reported on a SAP product with improved homogeniety and lower impurity levels called "Puroxal." This process involved ball-milling of a high-purity aluminum powder in aluminum ball mills and milling media using dimethylsilicone fluid as a lubricant. This resulted in greater oxide content control and lower iron and carbon impurity levels. Prior to extrusion into finished products, cold-pressed compacts of the milled and cleaned powder were given vacuum treatments at 600 to 625°C for 18 to 22 hours at 10^{-4} torr pressure. This treatment converted the amorphous aluminum oxide to the χ and η forms of aluminum oxide and resulted in finished products containing only 2 to 3 ppm hydrogen.

The Puroxal process was investigated along with other methods for production of experimental alloys in the present research, but it was not chosen. The strength and ductility of the product produced by the Puroxal process was similar to that achieved by other methods but results were not as reproducible for the small batches used in this investigation.

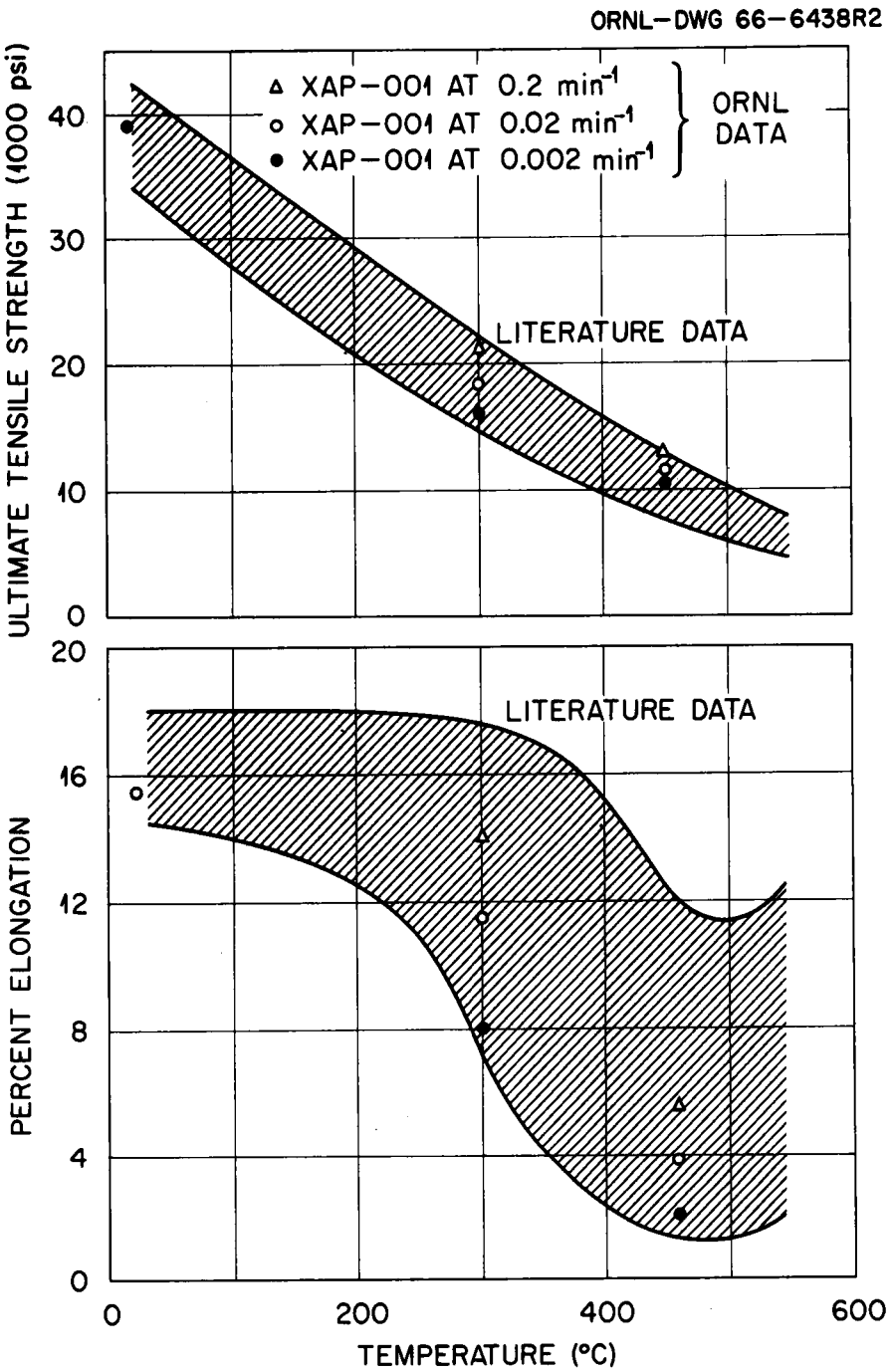

Figure 1. Tensile Strength and Ductility of XAP-001. Tested parallel to the extrusion direction. Hatched area represents scatter in reported SAP data. From Harman. (24)

Alloying Effects in Aluminum

The primary purpose of this investigation was to determine the effects of two types of alloying on the mechanical properties of aluminum dispersion strengthened with aluminum oxides: (1) an alloying element which increases the work hardening effect, and (2) alloying elements which produce stable intermetallic compounds. Magnesium was the obvious choice for the element to increase the work hardening rate. The elements chosen to produce intermetallic compounds were iron, molybdenum, zirconium, titanium, vanadium, and chromium. The individual effects of these alloying elements are discussed below.

Magnesium

Magnesium is the natural choice for alloying with aluminum to increase the work hardening rate because of its effective increase in the lattice parameter. Although there is decreasing solubility with decreasing temperature, alloys containing less than 7% magnesium are not normally heat treated and the major alloying effect is due to the solid solubility. Useful commercial wrought alloys contain from 1 to 7% magnesium. Useful commercial cast alloys contain from 4 to 10% magnesium with only those above 7% normally being used in the heat-treated condition. The utility of magnesium alloys below 10% is based on their good corrosion resistance, high strength without heat treatment, and good weldability. Heat treated alloys containing more than 10% magnesium show undesirable room-temperature aging and lowered resistance to stress corrosion cracking.

The solid solubility of magnesium increases from 2.1 atom % at 100°C to 18.9 atom % at 450°C. The aluminum-rich eutectic composition occurs at 37.4 atom % and the eutectic temperature is 450°C. The solid phases in equilibrium at this temperature are the aluminum solid solution containing 18.9 atom % magnesium and the Mg_2Al_3 phase containing 37.5 atom % magnesium. The Mg_2Al_3 phase melts at 452°C at very close to the ideal composition. Mg_2Al_3 has a complex face centered cubic structure with 1,173 atoms per unit cell and a lattice parameter of 28.13 Å. A transition phase forms from supersaturated solid solutions after long periods of heating at low temperatures. (25,26)

Iron

Iron forms a compound, $FeAl_3$, that is essentially insoluble in solid aluminum. (26) It usually appears as a coarse constituent in the microstructure of conventionally solidified alloys. However, the phase is very finely distributed in atomized powders due to the very high solidification rate. The $FeAl_3$ phase has a monoclinic structure with 100 atoms per unit cell. The lattice constants are a = 15.489 Å, b = 8.083 Å, c = 12.476 Å, and β = 107° 43 minutes.

The aluminum-rich eutectic occurs at about 0.9 atom % iron at 654 to 655°C. Iron is only slightly soluble in solid aluminum — 0.026 atom % at 655°C, 0.012 atom % at 600°C, 0.003 atom % at 500°C, and practically nil below 400°C (reference 26). This low solid solubility of iron in aluminum contributes to the stability of the finely distributed $FeAl_3$ compound in atomized alloy powders during further processing.

Molybdenum

The solubility of molybdenum in solid aluminum is very low: a maximum of 0.18 atom % has been reported at 660°C, other investigations indicated 0.11 atom % at the same temperature. (27) The compound in equilibrium with aluminum below 706°C is $MoAl_{12}$. Its structure is body centered cubic with a = 7.5815 Å.

Zirconium

The solid solubility of zirconium in aluminum is also very low — 0.068 atom % at 640°C, 0.041 atom % at 508°C, 0.033 atom % at 450°C, 0.024 atom % at 350°C, and 0.012 atom % at 20°C (reference 28). The compound in equilibrium with aluminum is Al_3. The structure is body centered tetragonal with a = 4.306 Å and c = 16,90 Å.

In small quantities, zirconium produces a grain refining effect in aluminum and its alloys. (25) It also provides a strengthening effect which levels off at about 1 atom %. In aluminum–copper alloys, zirconium increases the creep and fatigue properties at elevated temperatures when present with vanadium and manganese. Zirconium is used in welding wire to refine the grain and reduce weld cracking.

Titanium

The solid solubility of titanium in aluminum has been reported to be about 0.066, 0.048, and 0.042 atom % at 600, 500, and 400°C, respectively. (26) The compound in equilibrium with aluminum is $TiAl_3$. The structure is tetragonal with a = 5.435 Å, c = 8.591 Å, and c = 1.581 Å.

The primary use of titanium in aluminum is to refine the grain size. (25) It is especially effective in combination with boron. Titanium is also used in welding wire to refine the grain size and reduce weld cracking.

Vanadium

The solid solubility of vanadium in aluminum is 0.20 atom % at 660°C and less than 0.11 atom % at 500°C (reference 28). The most aluminum-rich compound reported is $Al_{21}V_2$. This compound has a cubic structure isotropic with $Mg_3Cr_2Al_{18}$ with a = 14.492 Å.

Chromium

The maximum solubility of chromium is 0.375 atom % at 660°C (reference 27). The aluminum-rich compound is $CrAl_7$ which has a very low solubility in solid aluminum and often appears as a coarse constituent in the matrix of normally solidified alloys. (25) The crystal structure of $CrAl_7$ is monoclinic with a = 20.47 Å, b = 7.64 Å, c = 25.36 Å, and β = 155° 10 minutes (reference 26). The only binary aluminum-chromium alloy currently used contains about 0.2 atom % and yields a gold color upon anodizing. About 0.15 atom % chromium added to aluminum-zirconium-magnesium-copper alloys improves the corrosion resistance and reduces stress corrosion cracking.

Previous Work on Alloying of Aluminum-Aluminum Oxide Dispersions

Alloying of the matrix in aluminum-aluminum oxide dispersions has been tried several times with the objective usually being increased strength rather than increased ductility at elevated temperatures. Irmann (29) alloyed magnesium and copper with SAP by blending elemental powders with ball-milled aluminum powder containing about 10% oxide. He reported increases in strength up to 200°C with a slight decrease at higher temperatures with no mention of ductility. Ito and Sawayanagi (30) blended 1 to 4% copper and 1 to 4% magnesium with a 4% oxide atomized powder (−150 +200 mesh). They found increased hardness and tensile strength up to 300°C. Ductility decreased with the alloy additions except for 300°C tests, where magnesium increased the elongation slightly.

Towner (6) has introduced some promising aluminum powder-metallurgy alloys which suggested the compound forming additions studied in this investigation. By compaction and hot extrusion of prealloyed atomized powders, he has produced alloys containing only 0.5% oxide which are stronger than 6% oxide SAP at temperatures up to 400°C after 100 hours at temperature. Atomization with resultant rapid quenching produces small and well-dispersed intermetallic precipitates in alloys containing the strong compound formers iron, nickel, zirconium, chromium, titanium, and vanadium. The primary strengthening agent in these alloys was $FeAl_3$. Prolonged temperatures above 400°C led to coarsening of the $FeAl_3$ and a decrease in strength. The total elongation of these alloys was around 10% at room temperature and increased with testing temperature in the manner characteristic of wrought aluminum alloys. This is in marked contrast to the oxide strengthened aluminum alloys which show a decrease in elongation with increasing temperature.

Russian workers (31) have studied oxide strengthened alloys containing 5% copper and 8% iron. They found improved strengths up to 200°C in blended copper alloys. They concluded that atomization of molten alloys was necessary to obtain strengthening benefits from low solubility elements such as iron. Neither blending of elemental powders of iron and aluminum nor pulverization of cast alloys gave positive results. They found the curve of strength versus temperature for 8% iron atomized alloy to be analagous to a 12% oxide alloy but lower at all temperatures.

Since this investigation began, three significant experiments with alloy modifications of oxide strengthened aluminum have been reported. Two of these reported the production of oxide strengthened alloys from aluminum powders containing magnesium. The third reported production of dispersion-strengthened alloys of aluminum with compounds other than Al_2O_3 introduced by blending.

Bufferd and Grant (32) produced oxide dispersion-strengthened alloys containing about 7 and 12% oxide from atomized aluminum powders with 1 to 5% magnesium. Their results are in agreement with those obtained in this investigation. The solid solution strengthening effect is additive to the dispersion strengthening up to temperatures of about 200°C. Above this temperature, the strength was comparable to unalloyed oxide dispersions of similar oxide content. They obtained room temperature ultimate tensile strengths up to 65,000 psi. In general, ductility decreased with increased magnesium or oxide content. Elongation values showed a maximum at about 150°C, then decreased with increasing temperature in a manner similar to unalloyed SAP.

Euratom workers (5) reported work on a SAP-type alloy made from an aluminum alloy powder containing 2 to 5% magnesium. X-ray diffractometry and chemical analysis showed the oxide particles to be made up of a spinel (Al_2O_3-MgO) and MgO, with no Al_2O_3. Their studies showed that the oxidation of magnesium takes place not only during ball-milling at room temperature, but continues during sintering at 600°C by reduction of Al_2O_3. Stresses leading to rupture in a given time during creep testing were about the same for these magnesium containing alloys as for unalloyed SAP of similar oxide content. However, the magnesium containing alloys showed higher elongation values for lifetimes of less than 500 hours. Elongation of 10% for 1-hour life and 5% for 50-hour life were reported and compare to about 1% elongation for unalloyed SAP. At lifetimes of 500 hours, elongations of 0.2 to 0.3% were the same for both types of alloys. The higher elongation values for the magnesium containing alloys were attributed to the lower frequency of micro-cracking observed at the particle-matrix interface.

Hansen (33) blended TiO_2, SiO_2, and Al_2O_3 with aluminum powders and compared their properties after consolidation at high temperature. In the aluminum-silicon oxide system most of the oxide phase was reduced and unsatisfactory properties were found. In the aluminum-titanium oxide system only a part of the oxide was reduced and increased elongation values were reported at equivalent strengths. The higher elongation was felt to be due to greater resistance of the oxide-matrix interface to crack formation.

CHAPTER III

DEVELOPMENT OF FABRICATION PARAMETERS

In order to determine the effects of alloying on the properties of SAP products, it was first necessary to develop fabrication techniques which produce uniform and reproducible rods for testing. Several methods were considered for introduction of oxide, consolidation into billets, and final extrusion into rods. The effects of the common impurities were also evaluated to determine to what extent they effect tensile properties and high-temperature stability of the product. When the optimum parameters were selected, a series of rods were produced with constant fabrication parameters to evaluate the reproducibility of the process. These process studies were performed using commercially available unalloyed aluminum powder. The fabrication process was scaled up to pilot plant proportions and the final product was compared to a commercial SAP of similar oxide content to verify the process.

Dispersion Preparation

The objective of dispersion preparation is to introduce the oxide uniformly and reproducibly. SAP is a typical example of a two-phase material whose properties depend principally on the distribution rather than the concentration of the second phase. Since the strength of dispersion-hardened material is inversely related to dispersoid spacing, (34) the distribution of oxide in the final product is the prime consideration.

Selection of Preparation Technique

The techniques that were considered to introduce the oxide with the desired distribution in the aluminum matrix are:

1. ball-milling of atomized powder,
2. controlled oxidation of atomized powder through the reaction with water at low temperature or with oxygen at reduced pressure and high temperature, and
3. mechanical blending of atomized aluminum and oxide powders.

The important characteristics of each of these methods are listed in Table 1. A comparison of their advantages and disadvantages led to the selection of ball-milling for dispersion preparation. The faults of the other approaches can probably be overcome by further development; however, an important consideration in this investigation was the fact that the technology of ball-milling large quantities of aluminum powder is established. Contamination, the main disadvantage of ball-milling, can be minimized by the use of relatively simple cleaning operations.

Determination of Ball-Milling Conditions

Several of the important variables in ball-milling were investigated, including materials of construction for the mill, grinding media, the types and amounts of surfactant and milling vehicle, and various factors associated with mill loading. Preliminary work used 10-inch-diameter by 10-inch-long aluminum alloy mill jars on a variable-speed mill rack. The process was then scaled up to pilot-plant size with a 36-inch-diameter steel mill.

TABLE 1

CHARACTERISTICS OF THE METHODS OF DISPERSION PREPARATION

Characteristics	Ball-Milling	Mechanical Blending	Controlled Oxidation	
			By Water	By Oxygen
State of technology	Well established	Not established	Not established	Not established
Contamination of product	Organics, H_2O, and iron	None	H_2O	None
Oxide, form[a]	Hydrated, low temperature	Stable, high temperature	Hydrated, low temperature	Stable, high temperature
Uniformity of distribution	Good	Poor	Good	Good
Reproducibility of concentration	Good	Best	Fair	Fair
Reproducibility of distribution	Good	Poor	Good	Good
Spacing achieved	Best	Poor	Poor	Poor

[a]The hydrated oxides formed at low temperature require conversion to anhydrous oxide for stability at service temperature.

During milling, it was found that a thin slurry promoted blending of the mill charge and enhanced uniformity of product. The loading factors for maximum efficiency for the pilot plant mill were:

1. ball volume, 33% of mill volume,
2. balls, 1/2-inch-diameter hardened steel,
3. aluminum powder, 4% of ball weight,
4. milling vehicle, mineral spirits (8% of ball weight),
5. surfactant, stearic acid (3% of aluminum powder weight).

Balls of both aluminum alloy 6061 and hardened steel (E52100) were evaluated for the milling operation. As illustrated in Figure 2, steel balls mill more efficiently and decreased the time required for a given oxide content; they also yielded a more uniform size distribution in the flake product. The use of hardened steel balls in a steel mill results in the inclusion of approximately 0.3% iron in the aluminum powder. This tramp iron was easily removed by passing the milled slurry through a magnetic filter. High-density alumina cylinders were tried, but they exhibited an unsatisfactory high self-attribution rate.

Stearic acid, oleic acid, or dimethylsilicone will prevent the agglomeration and welding together of SAP particles during ball-milling. The high cost of dimethylsilicone prohibits its large scale use. Stearic acid offers more protection to excessive oxidation in milling than does oleic acid. The lower oxide contents obtained for a given milling period, as shown in Figure 2, demonstrate the increased protection. Thus, more deformation is required to achieve a particular oxide content with stearic acid. Since the additional deformation produces a thinner flake and consequently a closer oxide spacing, stearic acid was selected as the best ball-milling surfactant for SAP powders.

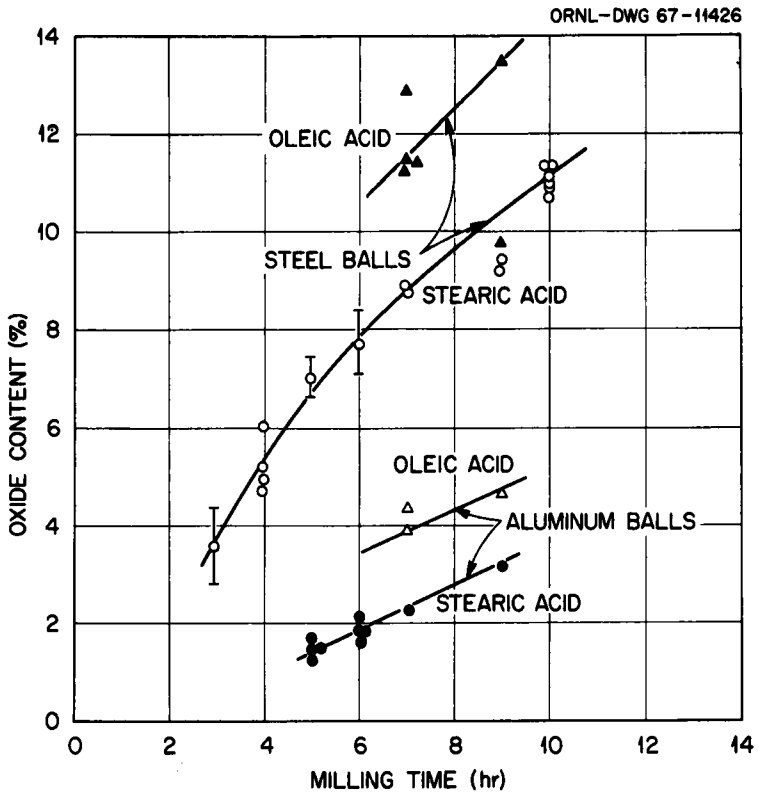

Figure 2. The Effect of Milling Time on Oxide Content of −100 Mesh Aluminum Powder. The I-bars represent the mean and estimate of standard deviation for six runs.

The ball-milling time required to obtain a given oxide content is longer for large powders than for very fine powders. Regardless of the milling period, the uniformity of the product for a particular oxide content appears to be independent of starting powder size. Nominally 20-μm size powders are considerably cheaper than the smaller powders and are also more readily available in quantities. Economical considerations, therefore, led us to select nominally 20-μm powder as ball mill feed material. An air-atomized nominally 16- to 20-μm powder is typically −100 mesh with 70% −325 mesh.

The milling period for a particular oxide content depends, among other things, upon the ball mill diameter and speed of rotation. The effect of mill diameter is shown in Figure 3. For constant milling conditions, the increase in oxide content is directly proportional to mill diameter. It was also found that the most effective milling speed is slightly less than that required to centrifuge the outer layer of balls. Lifter bars on the inside wall of the mill speeded the milling action by providing a mechanical lift for the balls and promoted reproducibility from batch to batch.

A major difference between this and commercial (23) milling practice for SAP powder is that in this investigation, sufficient surfactant was added to prevent welding of the powders during welding. The purpose of agglomerating the particles in commercial milling is to promote ease of handling and loading of dies for consolidation. However, it was found

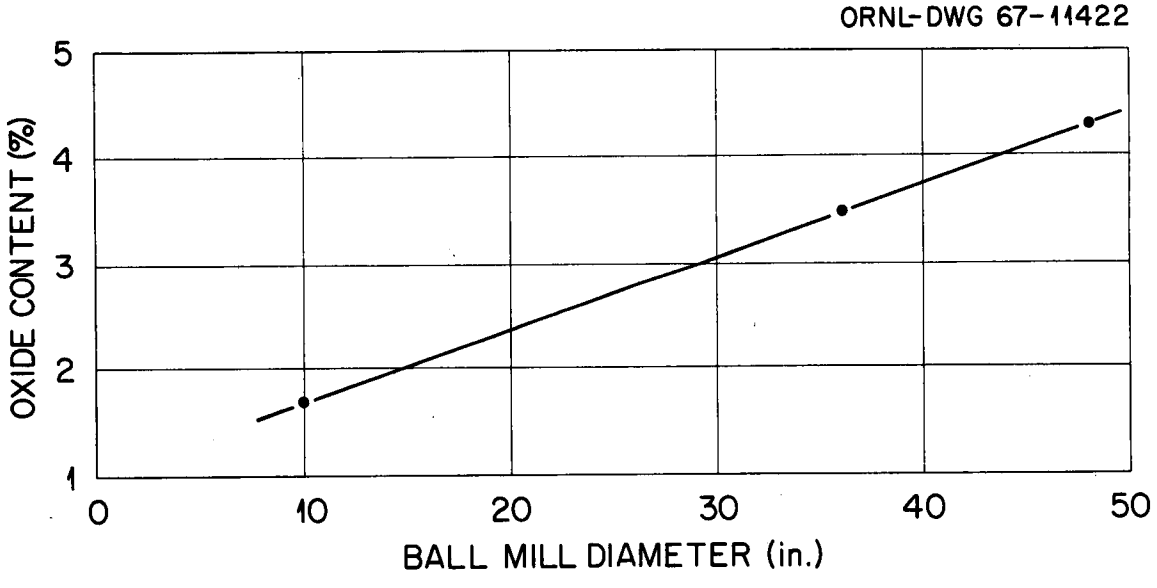

Figure 3. Effect of Mill Diameter on Oxide Content for Constant Milling Conditions.

that the oxide distribution was improved when the agglomeration was eliminated. To facilitate handling of this powder, the milled slurry was formed into a filter cake and vacuum dried at 300°C. The resultant product is easily broken into small clumps that are suitable feed material for subsequent consolidation.

Consolidation

The primary purpose of consolidation is to compact the SAP powder into a suitable billet for extrusion to a semifinished product with the aluminum oxide in a stable form of predictable morphology. Several combinations of cold pressing, vacuum annealing, vacuum hot pressing, and vacuum fusion were investigated to consolidate the powders. On the basis of superior mechanical properties with maximum homogeneity, vacuum hot pressing was selected for more detailed evaluation and scale-up to pilot production of SAP billets containing nominally 10% Al_2O_3. The investigation with larger billets included evaluation of the effect of consolidated density, vacuum annealing duration, and impurity levels of iron, carbon, and hydrogen on the uniformity and stability of the extruded product.

Stabilization of Oxide

The oxide layer on both atomized powder and ball-milled powder appears to be hydrated. X-ray diffraction patterns of the powders show only faint lines that correspond to bulk alumina hydrates. To more fully verify the presence of an alumina hydrate, it was found that gamma-type aluminas are insoluble in aqueous HCl, while α and β alumina trihydrates dissolve totally. Atomized and ball-milled powders are completely soluble

in aqueous HCl at room temperature. After high-temperature treatment, a residue is insoluble in aqueous HCl indicating at least some conversion to gamma-type alumina.

To determine the effect of vacuum heat treatment on the conversion of the hydrate to oxide and removal of ball-milling contaminants, ball-milled powder was subjected to vacuum thermogravimetric analysis.

The study included exposure of degassed materials to moist air at atmospheric pressure. Figure 4 shows the differential weight loss curve that was determined for a ball-milled powder containing 10% Al_2O_3 upon heating to 600°C at a rate of 100°C per hour; a commercial ball-milled flake behaved similarly.

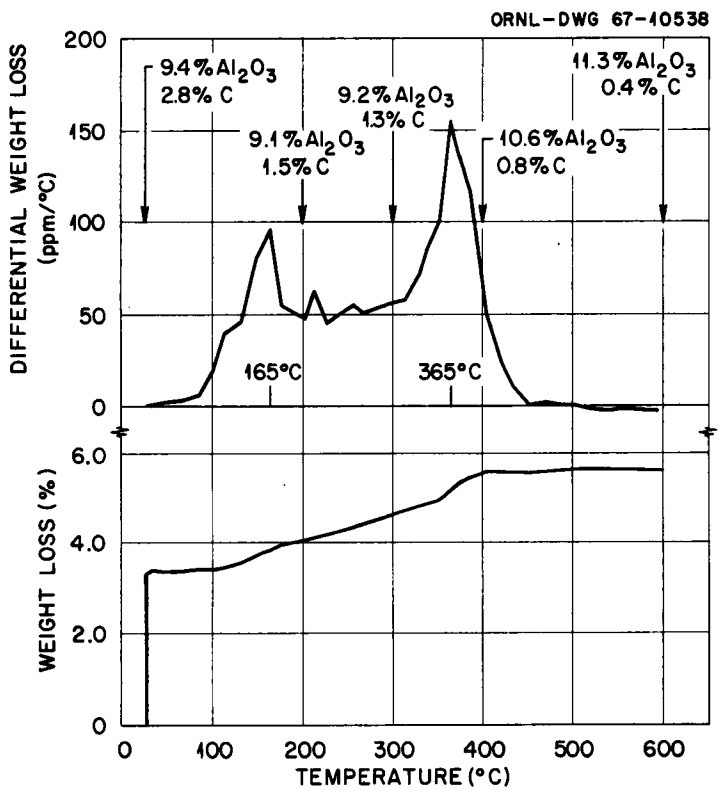

Figure 4. Effect of Temperature on Degassing Ball-Milled Aluminum Powder. The oxide and carbon contents were determined at the stages indicated. Atmosphere maintained at approximately 5×10^{-4} torr.

Before heating, the analytical system was evacuated to approximately 5×10^{-4} torr. The reduced pressure permitted approximately 60% of the total weight loss of 5.6% to occur during the pumpdown at room temperature.

In Figure 4 the peak shown at about 165°C results primarily from the release of loosely attached water and carbonaceous materials. Approximately half the carbon is released near this temperature. The alumina hydrate appears to decompose around 365°C, although some volatile hydrocarbons are still being released during this period of rising temperature. These results are in reasonable agreement with other data (35) which indicate that at 10 bars pressure, $Al(OH)_3$ transforms to AlOOH at about 100°C and AlOOH transforms to Al_2O_3 at 360°C.

When exposed to 11°C-dewpoint air, the degassed material gained weight, initially at the rate of 18 ppm per minute. The rate of weight gain decreased exponentially with time to about 0.5 ppm per minute at the end of 120 hours. The material lost approximately half this gained weight upon reheating to 600°C. Heating to above the melting point did not produce an additional weight change. Thus, it appears that water absorbed after vacuum annealing will be partially removed and partially converted to oxide and hydrogen by further vacuum annealing.

Dissolution of the heat-treated SAP powder in aqueous HCl at a maximum temperature of 65°C concentrates a sufficient quantity of Al_2O_3 for x-ray diffraction analysis. On material heated to 600°C, the χ and η phases of alumina were identified. Similar analyses on extruded SAP rods gave identical results.

Initial Processing Studies

Initially a series of 2-inch-diameter SAP billets were produced by six different processes from commercially supplied aluminum flake powder MP-3100* containing 6% Al_2O_3.

The compaction techniques and heat treatments are summarized in Table 2. The purpose of heating either the powders or the billets in vacuum was to convert the hydrate formed during ball-milling to an oxide that is stable at elevated temperatures and also to remove volatile contaminants as discussed above. Vacuum hot pressing was done in graphite dies at a maximum pressure of 1,600 psi. The procedure included holding the powder at 600°C for 2 hours and then pressing for 0.5 hour, all under vacuum. In vacuum fusion, cold-pressed compacts were heated at 700°C for 15 minutes or 1 hour. Immediately before extrusion all billets were 70 to 80% of theoretical density.

TABLE 2

BILLET CONSOLIDATION PROCESSES

Process	Powder Treatments			Billet Treatment	
	Vacuum Anneal[a]	Cold Pressing	Vacuum Hot Pressing[a]	Vacuum Anneal[a]	Vacuum Fusion[b]
A	---	Used	---	$<10^{-2}$	---
B	---	---	$<10^{-2}$	$<10^{-2}$	---
C-1	$<10^{-4}$	Used	---	---	---
C-2	$<10^{-2}$	Used	---	---	---
D	$<10^{-4}$	---	$<10^{-2}$	---	---
E-1	---	Used	---	---	15 min
E-2	---	Used	---	---	1 hour
F-2	$<10^{-2}$	Used	---	---	1 hour

[a]At 600°C. If used, pressure is given in torrs.

[b]700°C for time indicated in vacuum at below 10^{-2} torr.

*A product of Alcan Metal Powders, Inc., Elizabeth, New Jersey.

The billets were extruded with a reduction in area of 30 to 1 through a shear die at 435°C to 3/8-inch-diameter by 40-inch-long rods and subsequently straightened by swaging at 450°C with a reduction in area of 1.02 to 1. Data from tensile tests performed at 450°C and a strain rate of 0.0002 minutes^{-1} are shown in Table 3. Processes B and C produced material whose tensile strength depended significantly on specimen position. Oxide content and texture differences failed to account for the consistent decrease in strength along the rods. Although data were limited, material from processes E-2 and F-2 exhibited high oxide content near the nose of the extrusions, and their strengths varied similarly to those from processes B and C. Specimens that avoided the high-oxide areas yielded the tensile values presented in Table 3. In all processes, the uniform elongation was less than 2% at 450°C and the low strain rate. On the basis of the data presented in Table 3, process D appears to produce material of attractive strength and uniformity; the product closely approximates the properties of SAP 895,** which has a significantly higher oxide content.

Process B, however, is more easily adapted to production than is process D in that a solid billet rather than a low-density loose powder is vacuum annealed. Since the undesirable dependence of strength on sample location appears to be the only detriment of process B, both B and D consolidation routes were chosen for further evaluation and scale-up to pilot-plant-size billets 4 inches in diameter by 4 to 6 inches long.

**A product of Montecatini Edison SpA, Servizio Nucleare, Milano, Italy.

TABLE 3

EFFECT OF BILLET CONSOLIDATION PROCESS ON OXIDE CONTENT AND TENSILE STRENGTH OF EXTRUDED ROD

Consolidation Process	Oxide Content[a] (%)	Ultimate Tensile Strength[b] (psi)	Expected Deviation[c] of Ultimate Tensile Strength	
			(psi)	(%)
A	7.7–9.6	9,400	±650	6.9
B	6.6	12,200–55L	±960	8.6
C-1	8.2–9.4	13,700–39L	±1340	10.4
C-2	8.2–9.4	15,500–86L	±750	5.4
D	8.2	11,900	±820	6.9
E-1	8.5–11.5	11,900	(d)	(d)
E-2	8.5–11.5	11,500	(d)	(d)
F-2	10.1–14.3	10,900	(d)	(d)
SAP 895[e]	11.5	12,100	±770	6.4

[a]The range of values represents the maximum and minimum of at least four determinations along the rod length.

[b]If the strength varied significantly along the rod, it is given as a function of the distance L in inches from the nose of the extruded rod. Six samples with L from 4 to 40 inches were tested at 450°C and a strain rate of 0.0002 minutes^{-1}.

[c]Statistical tolerance limits calculated at the 95% confidence level to include 99% of a normal distribution.

[d]Insufficient tests to derive meaningful value.

[e]Values for commercial material.

Process Scale-Up

Processes B and D differ only in the sequence of the vacuum heat treatments used to stabilize the oxide. The procedure for the former is to vacuum hot press "as prepared" powder and then vacuum anneal the billets immediately before extrusion. In the latter the powder is heat treated before vacuum hot pressing. The problem in handling and

storage of vacuum-annealed powder and 80% dense billets is that adsorbed water may increase the hydrogen content of the extruded products.

The vacuum hot pressing procedures were the same for the larger 4-inch-diameter billets as for the 2-inch-diameter billets. Extrusion of the larger billets, however, required two stages. The primary extrusion was a reduction in area of 5.2 to 1 through shear dies at a billet temperature of approximately 500°C. The resulting 1.75-inch-diameter rod was then sectioned into several billets, and these were extruded at 435°C to a reduction in area of 30 to 1.

Processes B and D were compared in a series of 4-inch-diameter billets designed to establish the effect of initial billet density upon the mechanical properties of the extruded product. Because of the quantity of material required, two batches of commercial MD3100 flakes were used. Processes B and D billets were made, respectively, from powder containing 6 and 5% Al_2O_3. The annealed flake powder and the consolidated compacts were stored in sealed plastic bags to minimize rehydration.

Table 4 presents the strengths of the SAP rods extruded from the 4-inch-diameter billets of various densities. In general, processes B and D produced equivalent materials. The extrusions exhibited excellent uniformity of strength; the total expected variations are generally less than 7% of the average tensile values. Analysis of the tensile data showed no correlation of strength with either initial billet density or distance from the nose of the extrusions. The oxide content of the tensile specimens was also independent of their location along the rods.

TABLE 4

STRENGTH OF SAP RODS EXTRUDED FROM BILLETS OF VARIOUS DENSITIES

Rod	Consolidation Process	Billet Density (% of theoretical)	Oxide Content[a] (%)	Ultimate Tensile Strength[b]		
				Number of Determinations	Average Value (psi)	Expected Statistical Deviation[c] (psi)
239	B	71.5	8.0	18	11,010	±370
240	B	70.6	8.2	18	10,860	±370
241	B	80.6	6.5	18	10,490	±570
242	B	80.4	6.7	18	10,650	±570
243	B	86.7	6.5	18	10,450	±870
244	B	86.8	6.5	18	10,520	±780
245	D	79.8	5.4	18	10,320	±850
246	D	81.6	5.4	18	10,140	±340
247	D	91.8	5.3	18	10,250	±625
248	D	92.8	5.3	16	9,950	±625
249	D	98.2	5.9	12	10,160	±620
250	D	97.3	5.4	18	9,760	±620

[a]After primary extrusion.

[b]Test conditions: 450°C and a strain rate of 0.002 minutes^{-1}.

[c]Tolerance limits calculated at the 95% confidence level to include 99% of a normal distribution.

The extrusions from the 70% dense billets contain approximately 20% more oxide than the billets of higher density but exhibit the same level of strength. The additional oxide may be formed from the conversion of water of hydration during the billet vacuum anneal or from reaction with air before extrusion. This additional oxide only increases the thickness of the oxide layer around the aluminum flake. Since the interparticle oxide spacing is virtually unaffected, the strength of the material remains at the same level.

Tensile properties of commercial SAP and material from both B and D processes made from experimental flakes of 10% Al_2O_3 are compared in Table 5. The higher oxide content of the process B rods reflects the differences in primary extrusion conditions in that higher temperature and longer holding time of 80% dense billets before extrusion produced an additional increase in oxide content. The strength of rods produced by processes B and D are the same; however, process B extrusions exhibit better uniformity of strength. Process B extrusions also contain less hydrogen than the process D rods, in spite of precautions to prevent rehydration of the flake in process D. The rods from this experimental powder are 16% stronger than the SAP 895 of equivalent oxide content. Process B, in which the billet is vacuum annealed, is concluded to be the more desirable technique for consolidation of SAP powder for subsequent extrusion.

During the process selection, all vacuum treatments to stabilize the oxide were for 20 hours at 600°C. It is desirable to know the minimum duration at 600°C required during vacuum hot pressing and vacuum annealing to produce an extruded material that is stable at elevated

TABLE 5

EFFECT OF CONSOLIDATION ROUTE ON EXPERIMENTAL SAP RODS

Variables	Rods[a]				
	256	257	258	259	255 (SAP 895)
Consolidation route	B	B	D	D	---
Primary extrusion condition					
Preheat temperature, °C	600	600	500	500	---
Preheat duration, hours	2.7	2.7	2.1	2.2	---
Al_2O_3 content, %	12.1–12.3	12.5–12.6	11.3–12.0	11.3–11.6	11.3–11.5
Hydrogen content, ppm by weight	2	2	6	6	3
Mechanical properties[b]					
Ultimate tensile strength, psi	14,800	15,140	14,580	15,480	12,870
Standard deviation, psi	230	130	550	250	102
0.2% yield strength, psi	14,210	14,650	14,080	14,920	12,450
Elongation, %					
Total	0.90	0.79	0.87	1.16	1.74
Uniform	0.60	0.62	0.57	0.61	0.69

[a]Rods 256 through 259 are from experimental milled flake. Rod 255 is commercial SAP 895 received as 2 5/8-inch-diameter extruded (approximately 20 to 1) rod and subsequently extruded an additional 30 to 1.

[b]Test conditions: 450°C, 0.002 minutes^{-1} strain rate.

temperatures. Three 4-inch-diameter billets were preared by heating MD3100 flakes to 600°C in vacuum and immediately applying pressure until the density of the billet reached 80% of theoretical. The billets were then stored in sealed plastic bags until they could be annealed at 600°C in vacuum for 10, 17.5, or 25 hours. To prevent rehydration after the anneal, the billets were placed in a 600°C air-atmosphere holding furnace for primary extrusion without an intermediate cooling. Subsequent secondary extrusion by the normal procedure produced a total reduction in area of 156 to 1. The stability of the rods was determined by tensile testing six specimens of as-extruded material and six specimens of material that had been held at 600°C in vacuum for 40 hours. A previous process B extrusion was included to test the effect of eliminating the 2.5-hour holding period during pressing. The ultimate tensile strengths as extruded and the changes due to the stability tests are given in Table 6. The changes observed in all cases are small and are not significant with respect to normal variations. We conclude that the shorter vacuum hot pressing procedure with a 10-hour anneal of the 80% dense billets is sufficient for product stability. Shorter times should be investigated for process optimization.

TABLE 6

EFFECT OF BILLET VACUUM ANNEAL DURATION ON THERMAL STABILITY OF PROCESS B EXTRUSIONS

Rod	Rod Characterization		Vacuum Anneal Duration[a] (hour)		Ultimate Tensile Strength[b] (psi)	
	Oxide Content (wt %)	Hydrogen Content (ppm by weight)	Hot Pressing of Powder	Consolidated Billet	As Extruded	Change Upon Stability Test[c]
260-2	≅7.5	4.4	0.2	10.0	11,220	−320
261-2	≅7.5	3.4	0.2	17.5	10,640	−130
257-4	≅12.5	2.2	2.5	17.5	15,100	+120
262-2	≅7.5	3.0	0.2	25.0	10,760	−240

[a]Billets heated at 600°C for the indicated time in an atmosphere of less than 10^{-3} torr of air.

[b]Test conditions: 450°C and a strain rate of 0.002 minutes^{-1}; values represent the average of five or six determination.

[c]Stability test: extruded material held at 600°C in vacuum for 40 hours.

Effect of Impurities

During production, SAP becomes contaminated with three elements that could influence the uniformity and thermal stability of the material. Iron is included during ball-milling in the form of small particles from mill and ball wear. Carbon contamination results from the organic materials used as surfactant and vehicle during ball-milling. Hydrogen is produced by the decomposition of any aluminum hydrates or adsorbed water remaining after the billet anneal.

Hydrogen

High concentrations of hydrogen in SAP have been shown to cause structural instabilities at high temperature. (36) Hydrogen contents greater than 20 ppm generated fissures, voids, and external blisters in material exposed to temperatures of 600°C and above for several hours. To examine the effect of hydrogen at lower concentrations on thermal stability, the as-extruded strength of several rods were compared to the strength after annealing for 40 hours at 600°C in vacuum and in air. Table 7 shows the results. The vacuum heat treatment tended to lower the tensile strength, and, in all cases, reduced the hydrogen content to less than 3 ppm without evidence of blistering. Annealing in air also lowered the strength but it increased the hydrogen content. Blistering was observed in only one case – the air-annealed SAP 258-4, which contained 5.3 ppm hydrogen – and was accompanied by a significant decrease in strength. The most severe degradation of strength during vacuum annealing occurred in SAP 233, in which the hydrogen content was reduced from 25 to 2.5 ppm by the anneal. We note that the annealed strength of

TABLE 7

EFFECT OF HYDROGEN ON THE MECHANICAL PROPERTIES OF EXTRUDED SAP MATERIALS

Rod	Oxide Content (wt %)	Extrusion Billet Characterization		Hydrogen Content (ppm)		Heat Treatment Atmosphere	Average Ultimate Tensile Strength[c] (psi)		Average Uniform Elongation (%)	
		Consolidation Process	Diameter (inches)	As Extruded	After Annealing[a,b]		As Extruded	Change Upon Annealing[b]	As Extruded	After Annealing[b]
257-4	12.5	B	4	2.1	1.5	Vacuum	15,100	+120	0.643	0.573
262-2	7.0	B	4	3.0	1.6	Vacuum	10,760	−240	0.632	0.818
247-3	5.3	D	4	3.2	1.1	Vacuum	10,330	−610	1.115	0.876
261-2	8.1	B	4	3.4	2.0	Vacuum	10,640	−130	0.609	0.833
241-1	6.5	B	4	3.6	1.8	Vacuum	10,440	−40	1.004	0.745
255	11.4	Commercial SAP 895		3.6	1.5	Vacuum	12,870	−70	0.694	0.609
245-3	5.4	D	4	3.8	2.9	Vacuum	10,540	−760	1.330	0.757
260-2	7.1	B	4	4.4	1.3	Vacuum	11,220	−320	0.710	0.805
258-3	11.8	D	4	5.5	3.0	Vacuum	13,880	−110	0.698	0.763
233	6.1	D	2	25.0	2.5	Vacuum	13,080	−1990	0.952	1.420
257-2	12.6	B	4	1.8	5.0	Air	15,180	−370	0.620	0.550
258-4	12.0	D	4	5.3	7.7	Air	14,770	−1330	0.597	0.630

[a] Content is average of two to three determinations on actual tensile specimens.

[b] Rods annealed at 600°C for 40 hours in an atmosphere of less than 10^{-3} torr of air or 1 atmosphere of air.

[c] Test conditions: 450°C and a strain rate of 0.002 $minutes^{-1}$. Values represent the average of four to six determinations.

SAP 233 corresponds to material of similar oxide content but with lower initial concentrations of hydrogen. The uniform elongation was not significantly affected by the heat treatment or the hydrogen level. Hansen (37) has shown by creep testing that reducing the hydrogen content from 7 to 2 ppm in a SAP material with 7% Al_2O_3 had no effect on either the elongation or rupture life. We conclude that less than 5 ppm hydrogen in SAP is desirable for thermal stability of tensile properties.

Iron

The iron particles included during ball-milling react with aluminum at high temperatures. Electron microprobe analysis indicated qualitatively that the reaction product was composed of iron and aluminum in the proportions of $FeAl_3$. Five rods differing in tramp iron content were processed to determine if this reaction had any effect on the stability of mechanical properties. The iron content of milled flake powder was increased by blending with ball-milled iron powder. The 4-inch-diameter billets were consolidated and processed identically following process B. The powders were heated to 600°C in vacuum and pressure was applied until the billets reached 80% density. The billets were vacuum annealed at 600°C for 17.5 hours and then immediately extruded by the normal procedure to reduction in area of 156 to 1. To determine the thermal stability of the rods, the tensile strength at 450°C as extruded was compared to the strength after annealing 40 hours in vacuum at 600°C. The results of these tests are in Table 8. The changes in strength upon annealing are seen to be small and random with respect to iron content. The change in uniform elongation is a consistent decrease,

TABLE 8

EFFECT OF IRON ON MECHANICAL PROPERTIES OF EXTRUDED RODS

Rod	Chemical Composition[a] (wt %)				Mechanical Properties[b] at 450°C			
					Ultimate Tensile Strength, psi		Uniform Elongation (%)	
	Fe	C	Al_2O_3	H	As Extruded	Change Upon Anneal[c]	As Extruded	As Annealed[c]
				x 10^{-4}				
276	0.26	0.25	9.80	2.0	13,970	−70	0.78	0.69
272	0.57	0.21	8.23	1.8	12,480	+180	0.72	0.62
273	0.81	0.19	8.95	2.6	13,150	−390	0.78	0.57
274	0.97	0.25	8.84	2.4	13,100	−160	0.65	0.59
275	3.48	0.25	9.40	2.8	12,500	+40	0.57	0.37

[a]Samples taken adjacent to tensile specimens along rods. Al_2O_3 determined by gaseous HCl analysis.

[b]Strain rate of 0.002 minutes^{-1}. Values represent average of six determinations along two extruded sections.

[c]Specimens annealed in vacuum after machining. Conditions: 600°C, 10^{-3} to 10^{-4} torr, 40 hours.

which does not depend on iron content. Thus, these data indicate that iron as inclusions up to 3% has no significant effect on the magnitude or thermal stability of tensile properties of SAP rods.

Carbon

Much of the carbon in SAP is in the form of small inclusions, which are believed to be Al_4C_3. Electron microprobe analysis verifies that the composition of these inclusions is in the proportion of Al_4C_3. Since aluminum carbide decomposes readily in contact with water to produce hydrocarbon gas, the effect of the carbide inclusions in SAP on thermal

stability is of concern where moisture is present. To produce five rods differing in carbon content, finely powdered Al_4C_3 was blended with portions of a batch of experimental flake powder and processed into extruded rods in the manner used for the rods of varying iron contents. Sections of the rod were annealed at 600°C for 40 hours in vacuum and in air with an 11°C dewpoint. The results of tensile tests performed at 450°C on the extruded rod and after the stability tests are given in Table 9. The changes observed after the annealing are not significant with respect to normal variations and are random with respect to carbon content. These data indicate that carbon contents up to 2% in the form of Al_4C_3 inclusions are not detrimental to the magnitude or thermal stability of mechanical properties of SAP rods.

Process Evaluation

To determine the overall reproducibility of the process, extrusions from nine billets produced under the same conditions were evaluated. Nine 27-pound batches of aluminum powder were ball-milled for 20 hours by the reference process. A 4-inch-diameter by 4-inch-long billet from each batch was consolidated and extruded under the same processing conditions listed above for the rods of differing iron contents. Three specimens from each of two secondary extruded billets cut from along the two rods were tensile tested at 450°C. These results and the chemical composition of the rods are in Table 10. The strength within any particular billet was uniform. The maximum range observed was less than 2% of the mean. This amount of variation is similar to that observed in short, secondary extruded sections of SAP 895.

TABLE 9

EFFECT OF CARBON ON MECHANICAL PROPERTIES OF EXTRUDED RODS

Rod	Chemical Composition (wt %)				Mechanical Properties[b] at 450°C					
					Ultimate Tensile Strength (psi)			Uniform Elongation (%)		
	C	Fe	Al_2O_3	H	As Extruded	Change Upon Anneal in		As Extruded	As Vacuum Annealed[c]	As Air Annealed[d]
						Vacuum[c]	Air[d]			
				x 10^{-4}						
277	0.14	0.29	9.46	3.7	13,580	−180	−160	0.80	0.55	0.77
278	0.27	0.33	9.38	3.3	13,150	+70	−170	0.70	0.50	0.85
279	0.42	0.35	9.88	6.5	12,100	+700	+180	0.64	0.51	0.59
280	0.58	0.34	9.17	3.9	13,710	−370	−200	0.58	0.53	0.78
281	1.97	0.30	11.5	7.8	12,550	+610	−70	0.55	0.49	0.49

[a]Samples taken adjacent to tensile specimens along length of rods. Al_2O_3 determined by gaseous HCl analysis.

[b]Strain rate of 0.002 $minutes^{-1}$. Values represent average of six determinations along two secondary extruded sections per billet.

[c]Specimens annealed in vacuum after machining. Conditions: 600°C, 10^{-3} to 10^{-4} torr, 40 hours.

[d]Specimens annealed in moist air after machining. Conditions: 600°C, 1 atmosphere of air with 11°C dewpoint, 40 hours.

TABLE 10

COMPOSITION AND STRENGTH OF RODS FROM REPRODUCIBILITY STUDY

Rod	Ball Mill Run	Chemical Composition (wt %)				Mechanical Properties[a] at 450°C	
		Fe	C	Al_2O_3	H	Ultimate Tensile Strength (psi)	Uniform Elongation (%)
					x 10^{-4}		
276	23	0.26	0.25	9.80	2.0	13,970	0.78
277	27	0.29	0.14	9.46	3.7	13,580	0.80
282	20	0.28	0.22	10.1	1.7	14,640	0.54
283	21	0.22	0.24	9.48	1.7	14,130	0.58
284	22	0.30	0.30	9.35	2.4	13,800	0.62
285	28	0.32	0.26	8.35	2.3	13,110	0.60
286	29	0.40	0.22	9.70	2.1	14,230	0.70
287	30	0.33	0.32	8.50	2.2	13,300	0.68
σ, estimate of standard deviation		---	---	0.58	---	470	0.089
$\bar{X}$, mean		---	---	9.32	---	13,830	0.67

[a]Strain rate of 0.002 minutes^{-1}; values represent the average of six determinations along two secondary extruded billets.

The expected variations (3σ) among billets is ±10% of the mean. This spread in process reproducibility appears to be due to differences in milling, since the average strength correlates well with the oxide content. Further improvements in the billet-to-billet strength variations depends upon better control of the as-milled oxide content. Although comparable data have not been found for SAP 895, the allowed range of 9 to 12% Al_2O_3 would indicate strength variations similar to those observed in Table 10. The minimum strength value observed in the reproducibility study was 12,940 psi.

Figure 5 shows that the experimental SAP material is stronger than SAP 895 from room temperature to 550°C with similar uniform elongation. Note that each datum point in Figure 5 represents a single determination, except that at 450°C, which is an average of six specimens tested at an earlier date.

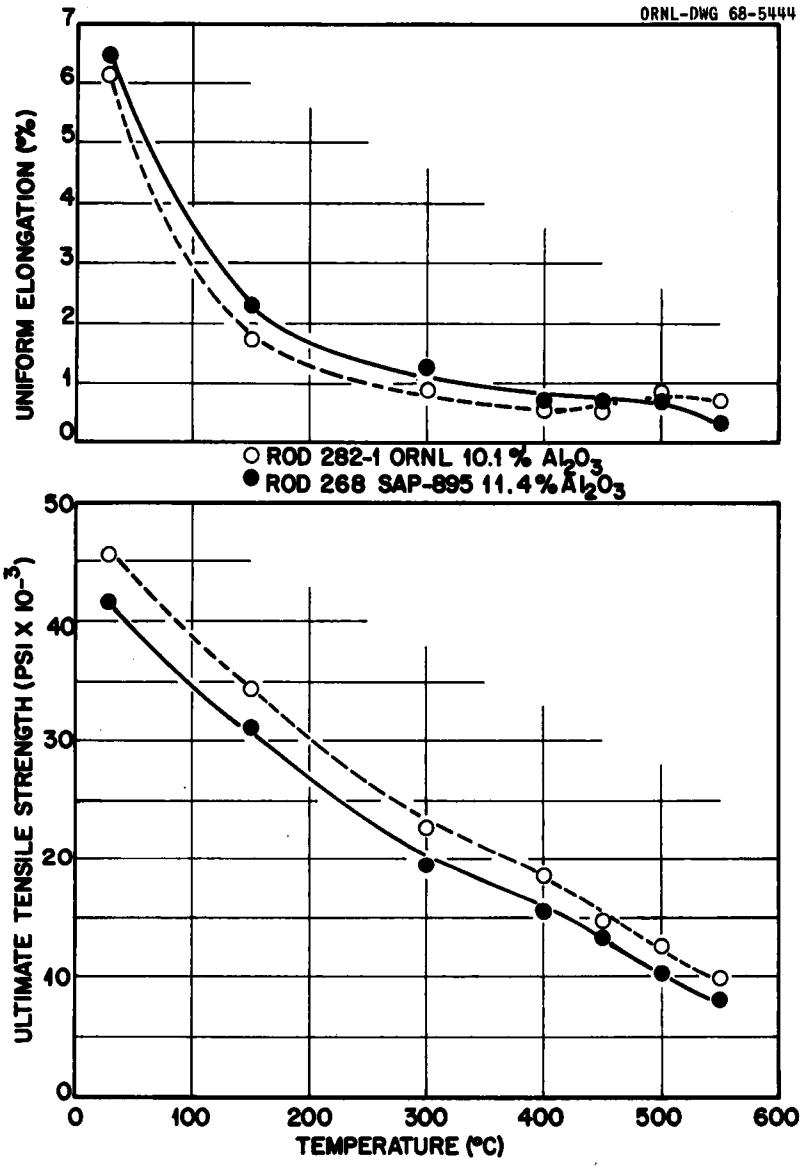

Figure 5. Strength and Uniform Elongation of Experimental SAP and Commercial SAP 895 as a Function of Testing Temperature. The strain rate was 0.002 minutes^{-1}.

The internal structures of the experimental material and SAP 895 may be compared by conventional metallography in Figure 6 and by transmission electron microscopy in Figure 7. In viewing the photographs, one should be aware that SAP 895 has received a total reduction in area of approximately 510 to 1 in comparison to 156 to 1 for the experimental material. This additional hot working should have resulted in slightly improved oxide distribution and corresponding increase in strength. The excellent uniformity and closer spacing of the oxide in the experimental material accounts for its higher strength at a given oxide concentration. The better oxide distribution appears to result from the elimination of intentional agglomeration of individual particles during ball-milling. Commercial SAP milling practice welded the particles together, (23) whereas, sufficient surfactant and milling vehicle were used in the experimental milling to maintain individual flake particles.

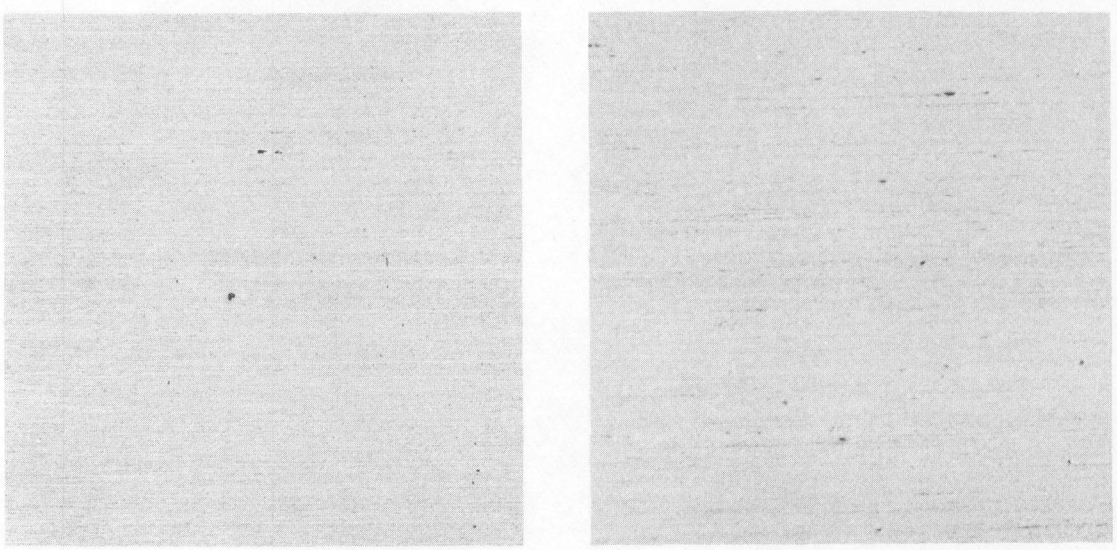

Figure 6. Comparison of Longitudinal Microstructure (100X) of Experimental SAP (right) and SAP 895 (left). Etched in 1% HF.

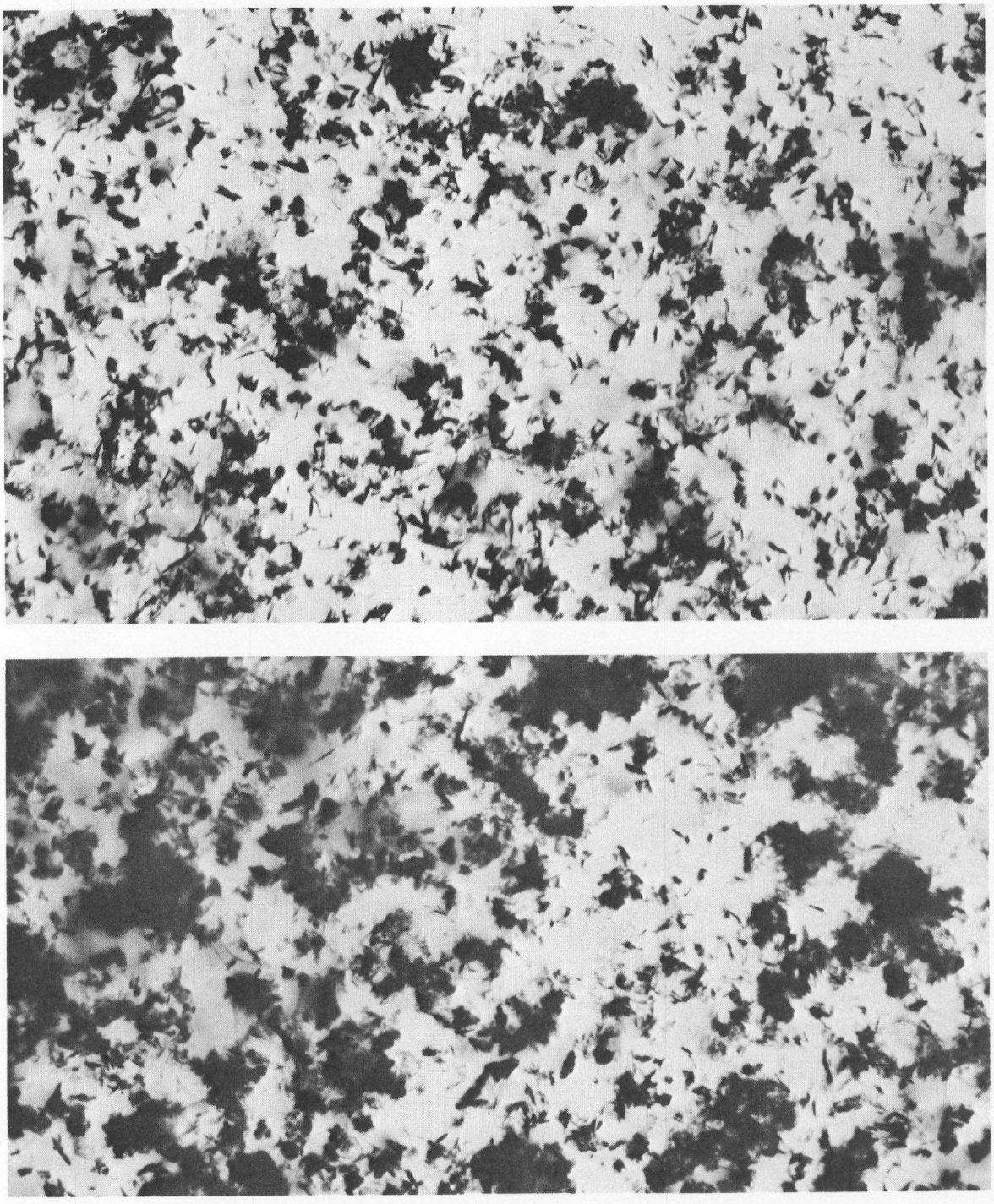

Figure 7. Comparison of Transmission Electron Microstructure (25,000x) of Experimental SAP (top) and SAP 895 (bottom). Transverse section.

CHAPTER IV

PRODUCTION OF ALLOYS

The general processing steps in the production of dispersion-strengthened aluminum alloys are: preparation of powders, oxidation, consolidation, heat treatment to convert the oxide to a stable form, and extrusion. The alloys for this experiment were processed using parameters developed for unalloyed dispersions described in the previous chapter and found to produce uniform and reproducible products (process B). The production of the alloyed powders and specific fabrication details are discussed in this chapter.

Powder Production and Characterization

Atomization of molten alloys proved to be the only way to obtain powders fine enough for ball-milling (−100 mesh) with a uniform fine distribution of the low solid-solubility elements. Other methods, such as mechanical disintegration of chill-cast alloys, resulted in intermetallic compounds too large to be of benefit for strengthening. Atomized alloy powders of the desired composition are not available commercially. Through a cooperative program with the Illinois Institute of Technology Research Institute, procedures were developed for air atomization of molten alloys such that an appreciable fraction of −100 mesh powders was obtained. The powders were collected in a water bath. After the powders settled, the water was decanted. The powders were then collected, washed with acetone, and dried. The resultant oxide content of about 0.5% for the atomized powders was about the same as that observed after air atomization and collection of aluminum powders.

Ten-pound ingots of each alloy were prealloyed by induction melting in graphite crucibles for the aluminum-magnesium alloys and by arc melting for the compound forming alloys. Four additional ingots were prepared for the aluminum-4% magnesium and the CA-0219 alloy to use in determining the optimum atomization conditions.

The atomized powders were irregular to spherical in shape. The particle size distributions are shown in Table 11. The chemical analysis of the -100 mesh fraction determined by spark source mass spectroscopy is shown in Table 12.

TABLE 11

SCREEN ANALYSES OF ATOMIZED POWDERS

Ingot Number	Wt % in Given Size Range		
	+40 mesh	-40 +100 mesh	-100 mesh
M-7	6.7	22.1	71.2
M-2	17.2	29.5	53.3
M-6	32.0	33.5	34.5
CA-0219	11.6	29.2	59.2
CA-0224		21.4[a]	78.6
CA-0223	7.5	10.0	82.5
CA-0218	34.5	16.6	48.9
CA-0222	36.2	25.2	38.6

[a]+100 mesh.

TABLE 12

CHEMICAL CONTENT OF ATOMIZED POWDERS

Ingot Number	Chemical Content,[a] wt %						
	Mg	Mo	Fe	Zr	Ti	V	Cr
M-7	2.0						
M-2	4.3						
M-6	6.2						
CA-0219		3.8	0.09	0.7	0.034	0.058	0.056
CA-0224		4.9	1.7	0.24	0.09	0.046	0.054
CA-0223		4.1	4.1	0.25	0.12	0.02	0.33
CA-0218		2.1	0.07	2.4	0.13	0.076	0.25
CA-0222		4.4	1.7	1.4	0.064	0.037	0.83

[a]Determined by photoelectric analysis of spark source mass spectrography. Precision ±10%.

Production of Alloy Rods

The procedures used in production of rods from the alloyed powder were held constant for all alloys. This procedure is essentially Process B as discussed in the previous chapter. A flow diagram for the entire process is shown in Figure 8. Temperatures for the magnesium containing alloys were limited to 550°C because of the lower melting points.

The oxide content of −100 mesh alloyed powders resulting from the ball-milling as a function of milling time is essentially the same as that for unalloyed powders shown in Figure 2, page 25, for steel balls and stearic acid lubricant. There was more scatter in the oxide content data for the alloyed powders due primarily to differences in handling times for the milled powders prior to analyzing for oxide content. Oxide content can increase after ball-milling and prior to final extrusion

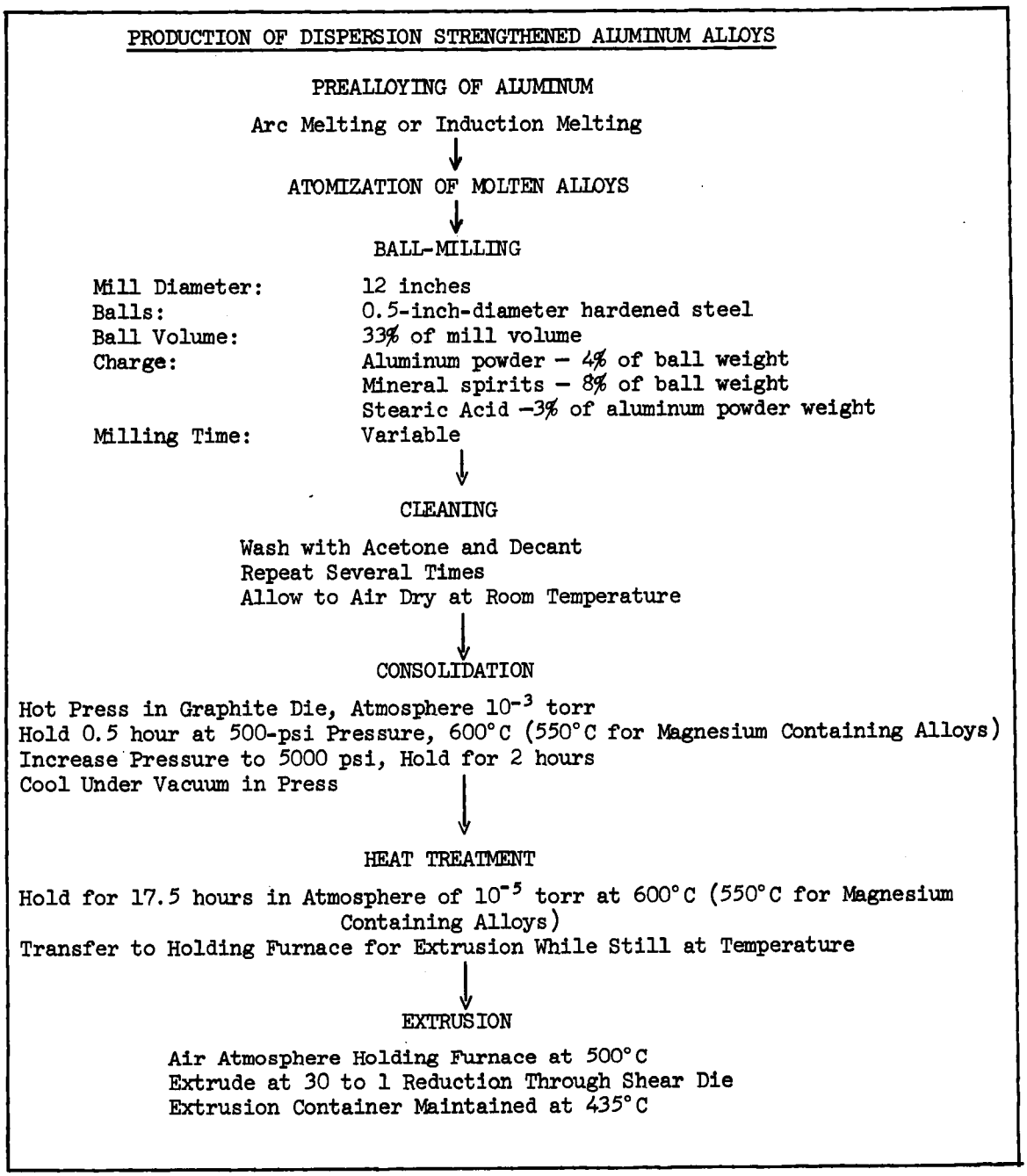

Figure 8. Outline of Procedure for Production of Experimental Dispersion Strengthened Aluminum Alloys.

due to exposure to air and moisture. However, the additional oxide does not contribute to strength since it merely increases the thickness of the oxide particles and essentially does not change their spacing. The oxide spacing is primarily determined by ball-milling time (i.e., aluminum flake thickness obtained during milling). Since strength is controlled by oxide spacing, strength correlates better with ball-milling time than with oxide content of the final extruded rod. Thus, ball-milling time for the alloyed powders is used as the method of correlating the different alloys in this study.

CHAPTER V

EVALUATION PROCEDURES

Tensile Testing

The elongation and strength of dispersion-strengthened aluminum are influenced by test temperature and strain rate of testing. These parameters were carefully controlled during the tensile tests. Specimens were machined from the extruded alloy rods to the dimensions shown in Figure 9. Chromel-P–Alumel thermocouple wires are resistance welded to both specimen grips very close to the gage length of the specimen. These thermocouples control a two-zone temperature-control system utilizing separate power controllers coupled with Speedomax H temperature recorders. Both thermocouples are periodically monitored manually with a potentiometer to assure that both grips are reaching the same temperature and within

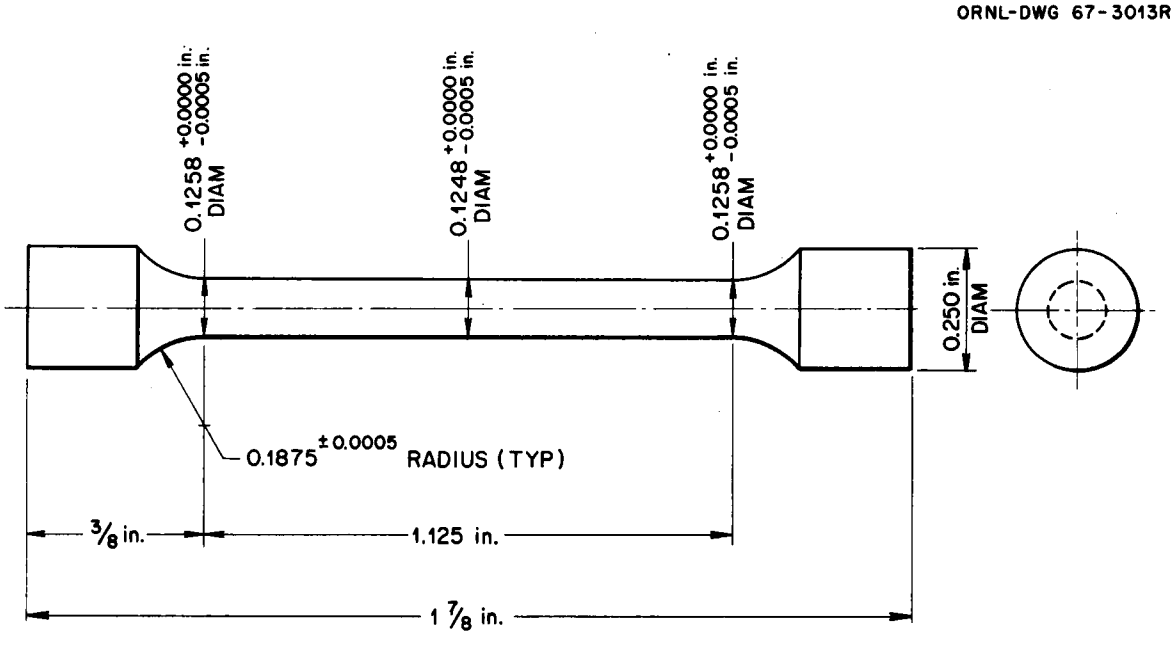

Figure 9. Tensile Specimen.

±3°C of the desired temperature. Typical time required for heating to 450°C was 10 minutes. The specimen was then held at test temperature for 10 minutes prior to starting the test to assure that the temperature was uniform. The tensile test setup used is shown in Figure 10 (thermocouples are not shown in this photograph).

The tensile tests were run in an Instron Universal Testing Machine at a constant crosshead speed of 0.02 inches per minute. This is equivalent to a strain rate of 0.02 minutes^{-1} for a 1-inch gage length specimen. The tensile properties were obtained from a plot of load versus crosshead movement plotted by the Instron from the load cell signal and gear drive movement. These tensile testing procedures have been shown to provide consistent and reproducible tensile test data for dispersion-strengthened aluminum. (24)

Oxide Content Determination

The oxide content of the extruded alloys was determined by fast neutron activation analysis. The samples (generally tensile specimens after testing) were bombarded with fast neutrons from a source. The activation of the oxygen in the sample is determined and compared with a standard. The oxygen content is determined very accurately and quickly by this method. The precision of the method is ±10% of the reported value in the range of 1 to 15% Al_2O_3.

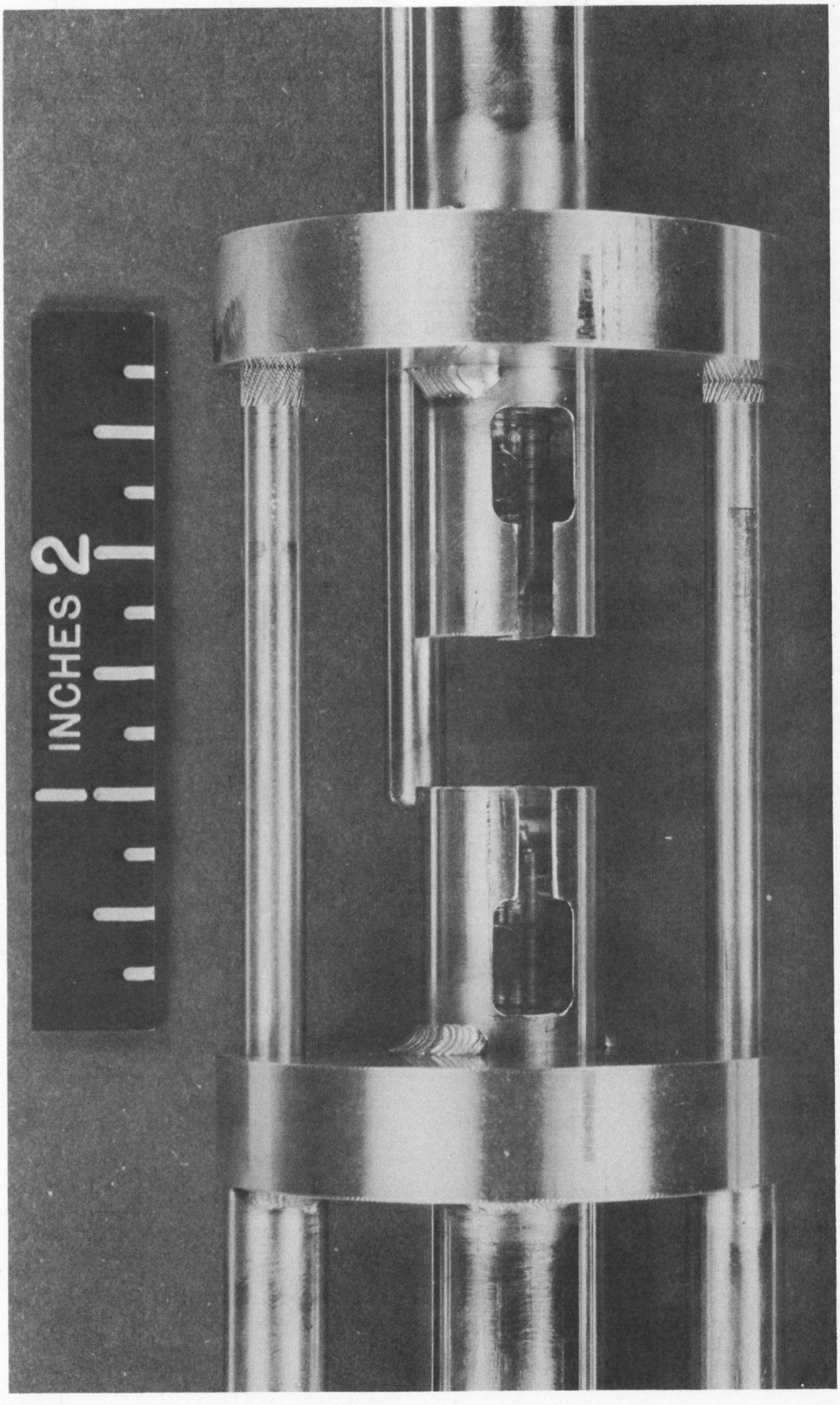

Figure 10. Pull Rod Setup for Elevated Temperature Tensile Testing of SAP.

Transmission Electron Microscopy

Each alloy type was examined by transmission electron microscopy on a Hitachi HU-200 electron microscope operated at 200 kilovolts. The thin foils for examination were prepared in a three-step process following largely a technique developed by DuBose and Stiegler. (38) The procedure consists of initial electrolytic jet dimpling in a perchloric acid solution, chemical smoothing treatment in a hot solution of phosphoric acid, and finally electrolytic penetration in another perchloric acid solution.

Optical Metallography

Conventional metallographic examination was performed on all alloys. The samples were mounted in epoxy, ground, and then polished vibratorily using Linde B alumina. Etching was accomplished by swabbing with a 1% HF solution. The samples were examined and photographed using a Bausch and Lomb research metallograph.

CHAPTER VI

RESULTS

The room temperature properties of SAP-type alloys can be significantly improved by alloy additions as shown by representative data in Figure 11. Tensile strengths up to 77,000 psi were obtained with the 6% magnesium additions which is in the range of the strongest conventional aluminum alloys. The additional dispersion strengthening due to the intermetallic compounds (alloy CA-0222) is effective from no ball-milling up to 12 hours ball-milling time. The magnesium additions, however, are more effective at the lower ball-milling times. As shown in Figure 12, the dispersion strengthening by intermetallic compounds is additive to the oxide strengthening even at 450°C. The magnesium additions slightly decrease the strength at 450°C. The uniform elongation at 450°C drops to a low value after only 2 hours ball-milling. This is the minimum amount of ball-milling which results in a worthwhile increase in high-temperature strength. Even at this low oxide content, there is early void initiation at oxide agglomerates which results in extremely low uniform elongation values at high temperatures. This is discussed further in the following chapter. Thus, decreasing the oxide content (i.e., decreasing ball-milling time) is not a practical method for improving uniform elongation at elevated temperatures.

The effect of the magnesium additions on tensile strength and ductility is shown in Figures 13 through 16 for samples given either no ball-milling or 2 hours ball-milling. The magnesium additions are effective in strengthening the alloys at room temperature and 200°C,

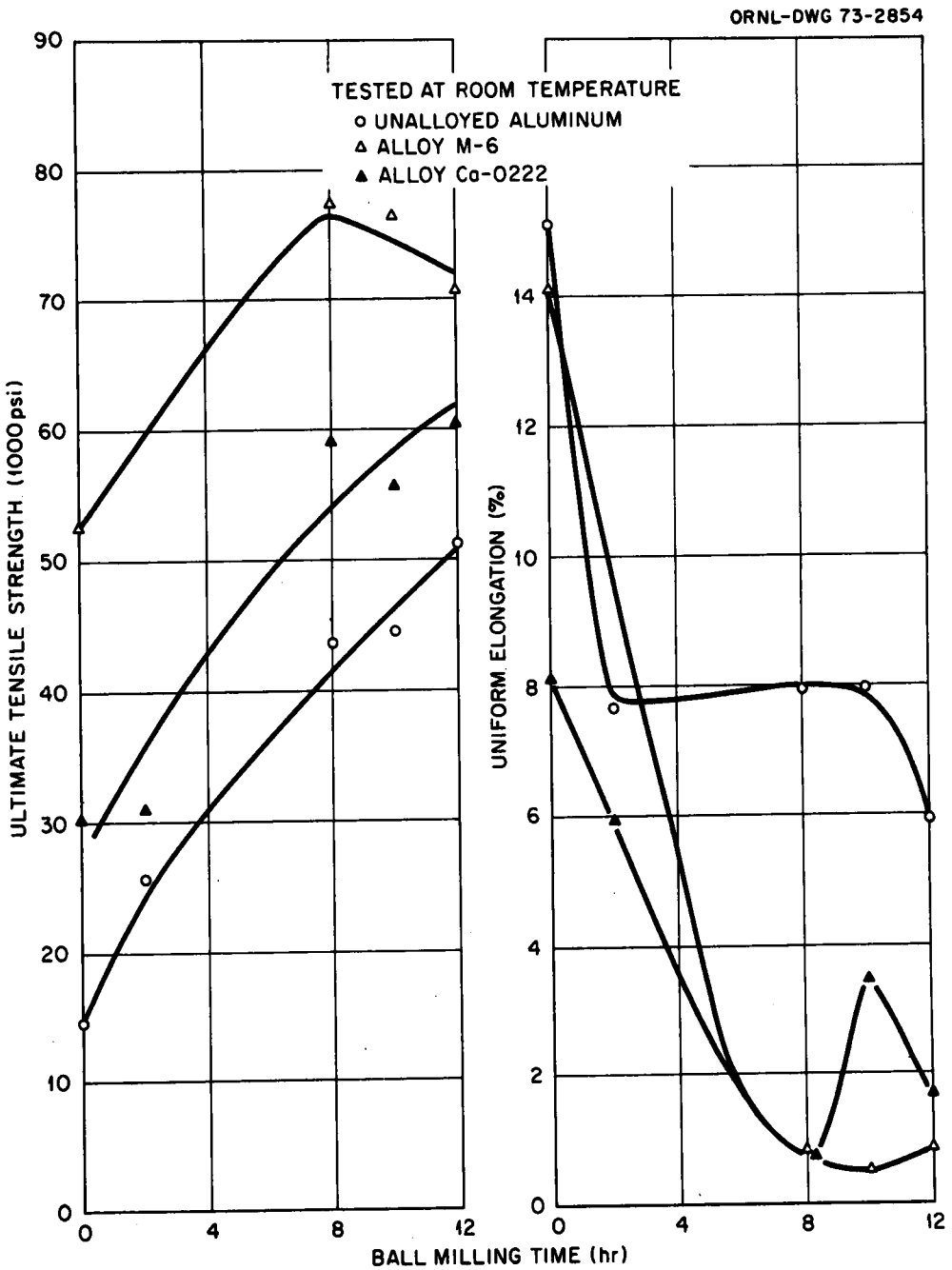

Figure 11. Room-Temperature Tensile Properties of Representative Experimental Alloys as a Function of Ball-Milling Time.

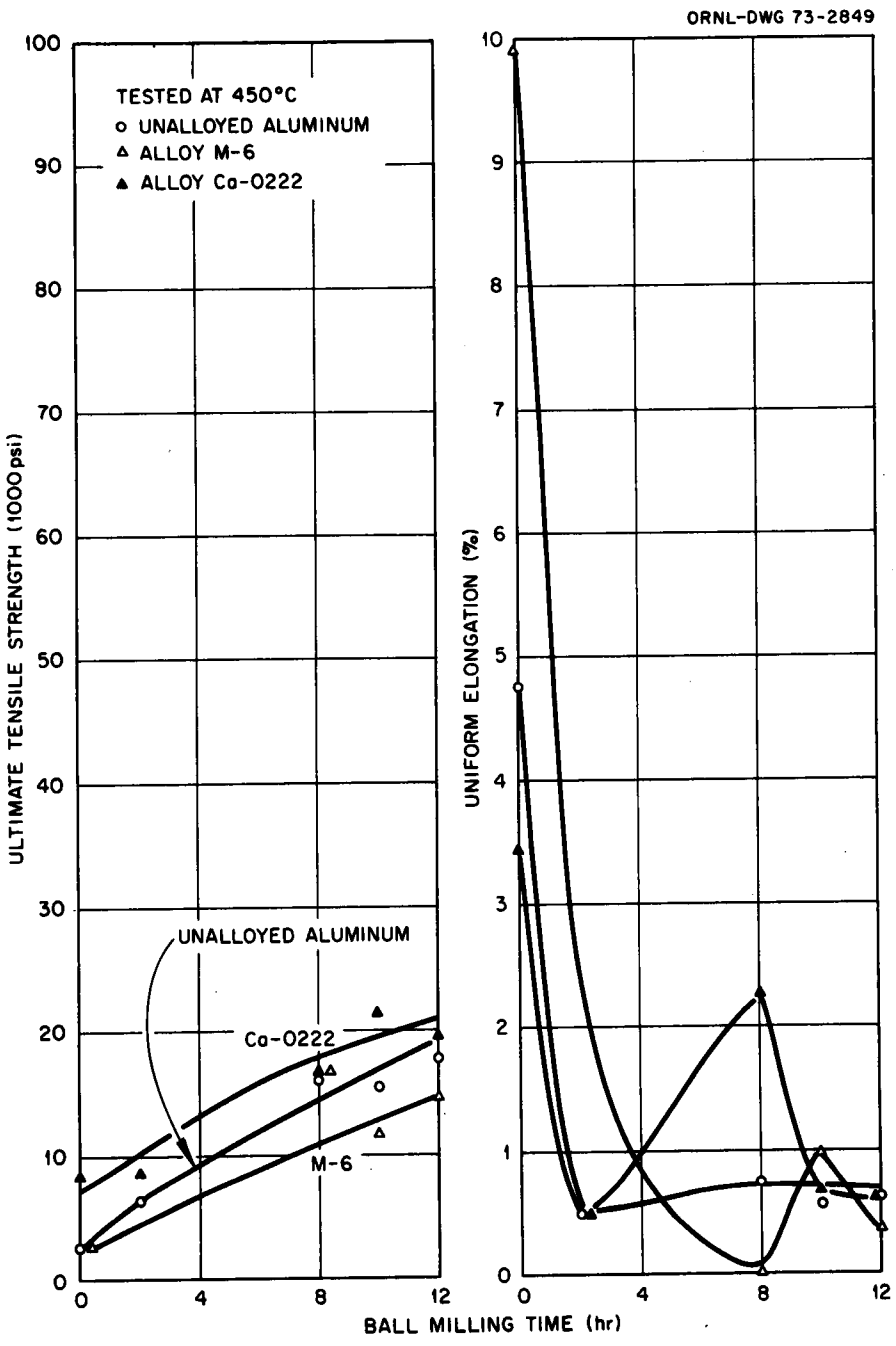

Figure 12. Tensile Properties at 450°C of Representative Experimental Alloys as a Function of Ball-Milling Time.

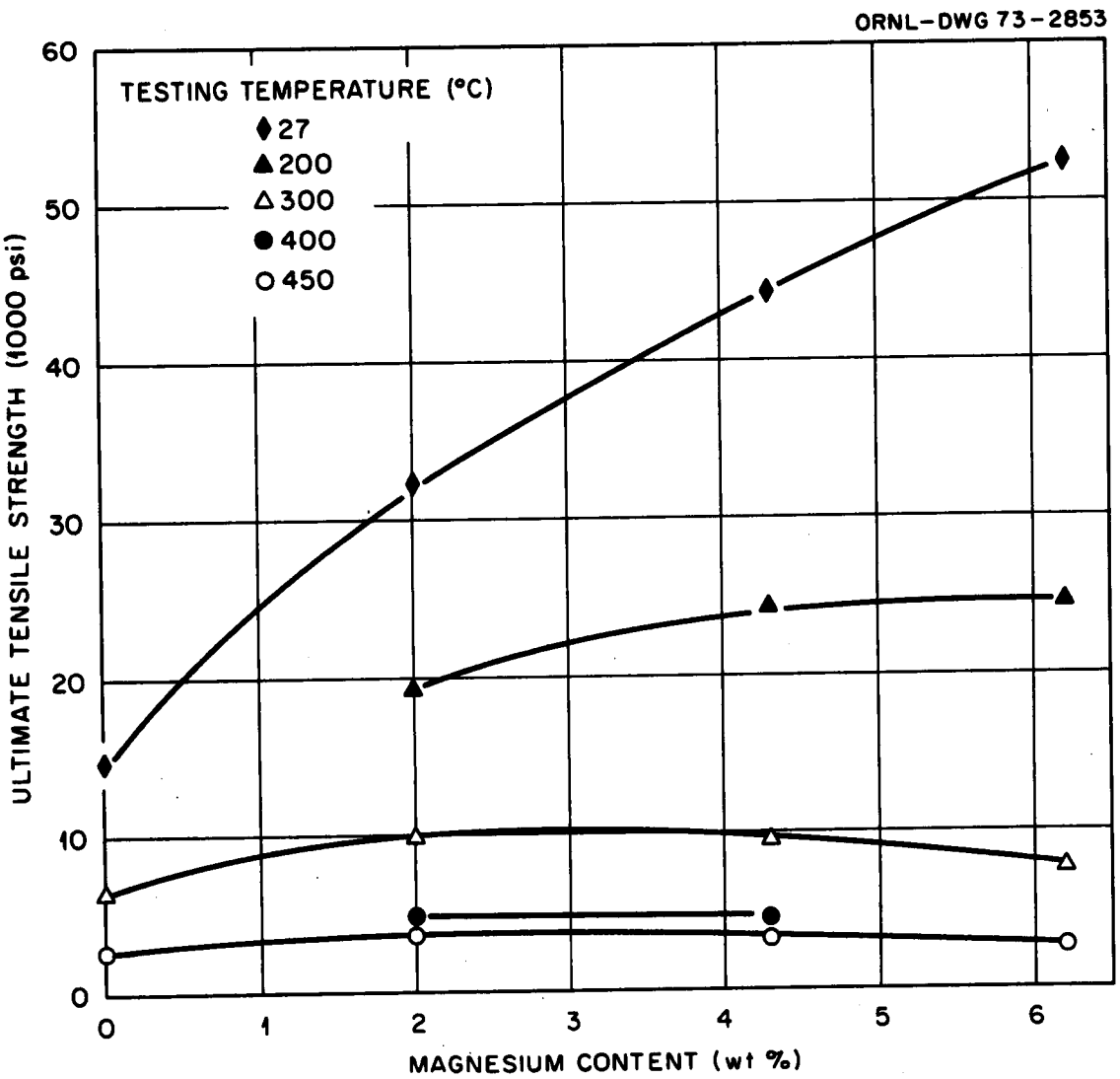

Figure 13. Tensile Strength of Experimental Magnesium Alloys With No Ball-Milling.

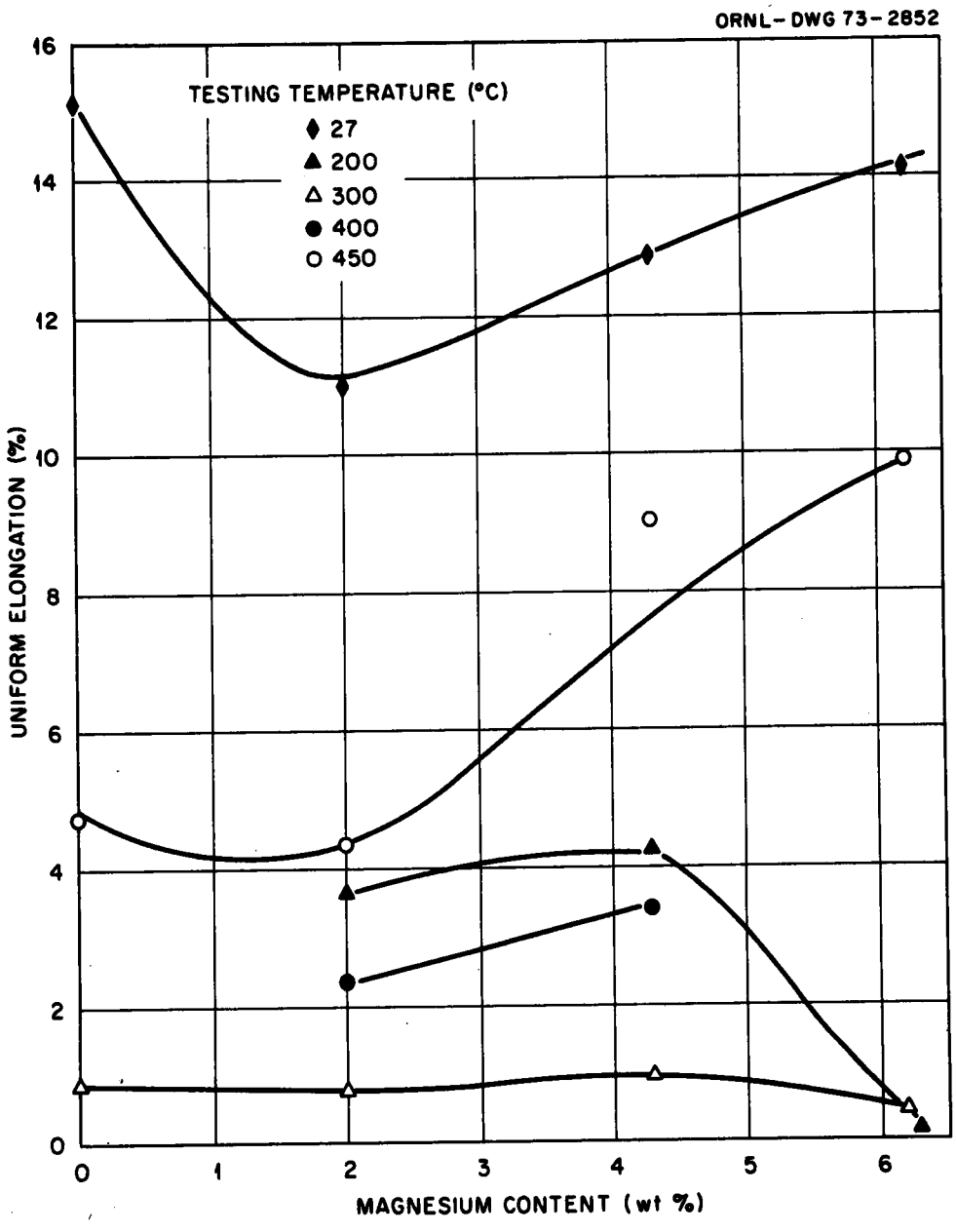

Figure 14. Uniform Elongation of Experimental Magnesium Alloys with No Ball-Milling.

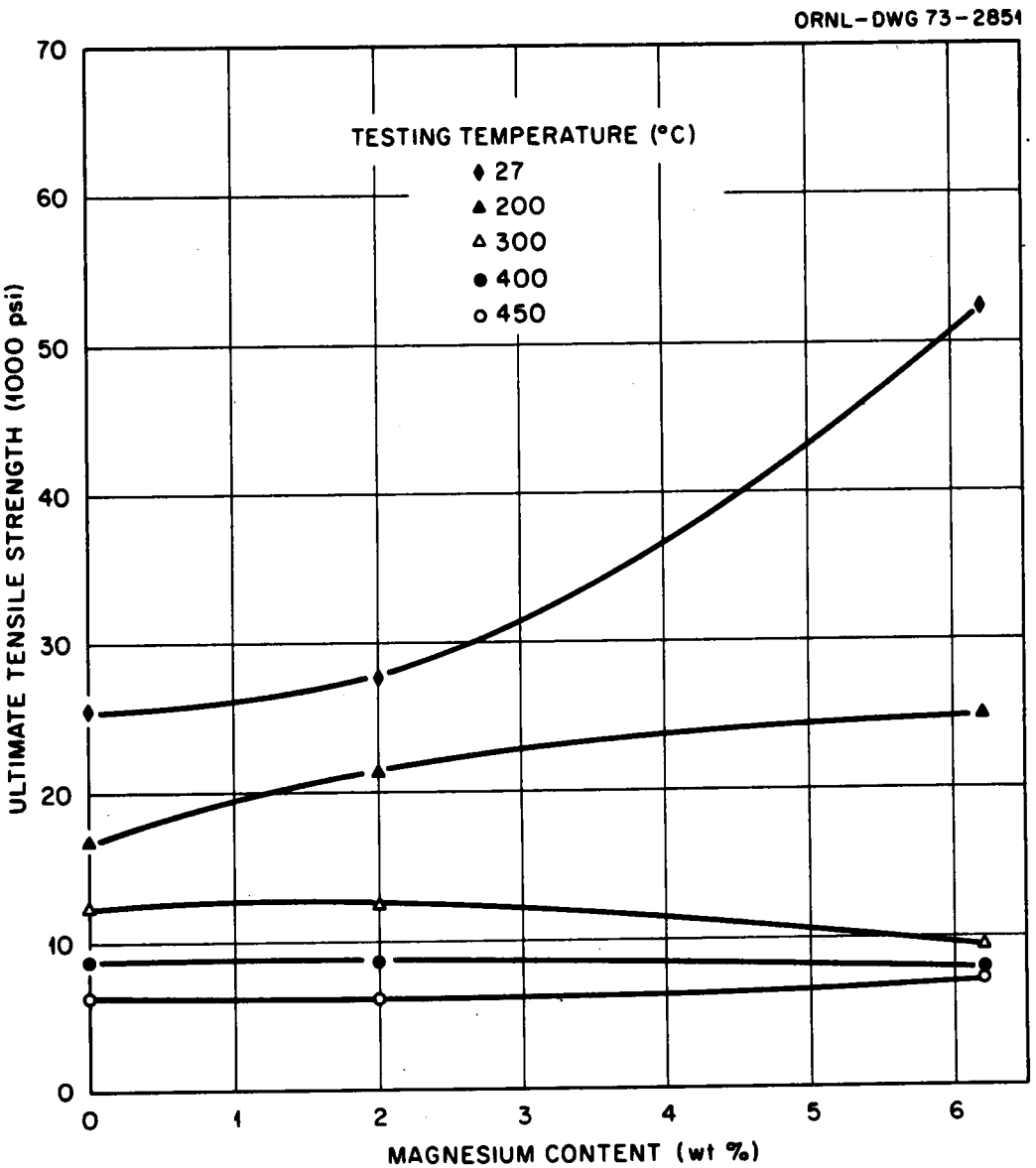

Figure 15. Tensile Strength of Experimental Magnesium Alloys with 2 Hours Ball-Milling.

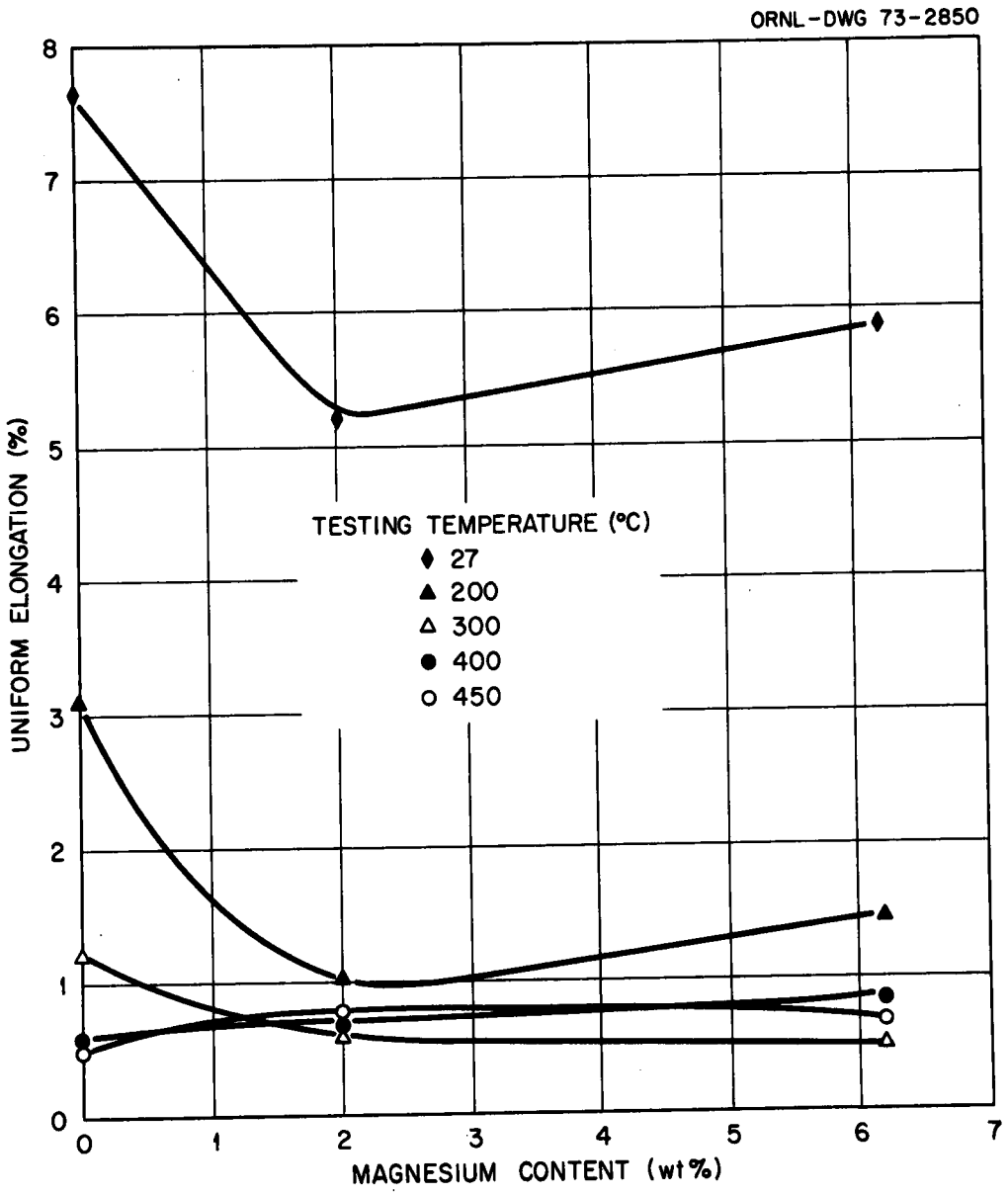

Figure 16. Uniform Elongation of Experimental Magnesium Alloys with 2 Hours Ball-Milling.

but not at 300°C and higher temperatures. These observations agree with those of Bufferd and Grant (32) who have published the tensile properties of oxide dispersion-strengthened aluminum-magnesium alloys at temperatures up to 300°F since this investigation was begun.

In contrast to precipitation or work hardened alloys, the dispersion hardened aluminum-magnesium alloys retain their high room-temperature strength after being heated to high temperatures. If, however, the alloy is strained at high temperatures, the subsequent room-temperature strength will be lowered due to the initiation of cavity formation as will be discussed in the next chapter.

The strength and elongation of dispersion-strengthened alloys ball-milled 10 hours are shown in Figure 17. The atomized alloy CA-0222 is compared with unalloyed aluminum. The alloy CA-0222, which is further dispersion strengthened by the intermetallic compounds, is seen to have higher strength at all testing temperatures with a slight decrease in total elongation and a slight increase in the uniform elongation at 450°C.

The tensile properties of several alloys strengthened by intermetallic compounds are shown in Figure 18 and compared to unalloyed aluminum. These alloys were produced from as-atomized powders with no ball-milling. Several of the alloys have tensile strengths about half that of a typical SAP alloy at 450°C and have much higher elongations. The very low solid solubility of the alloying elements in aluminum promotes the high-temperature stability of the strengthening effect of the dispersed compounds. Towner (6) has shown that no degradation of tensile properties of similar alloys occurred after 100 hours at 400°C.

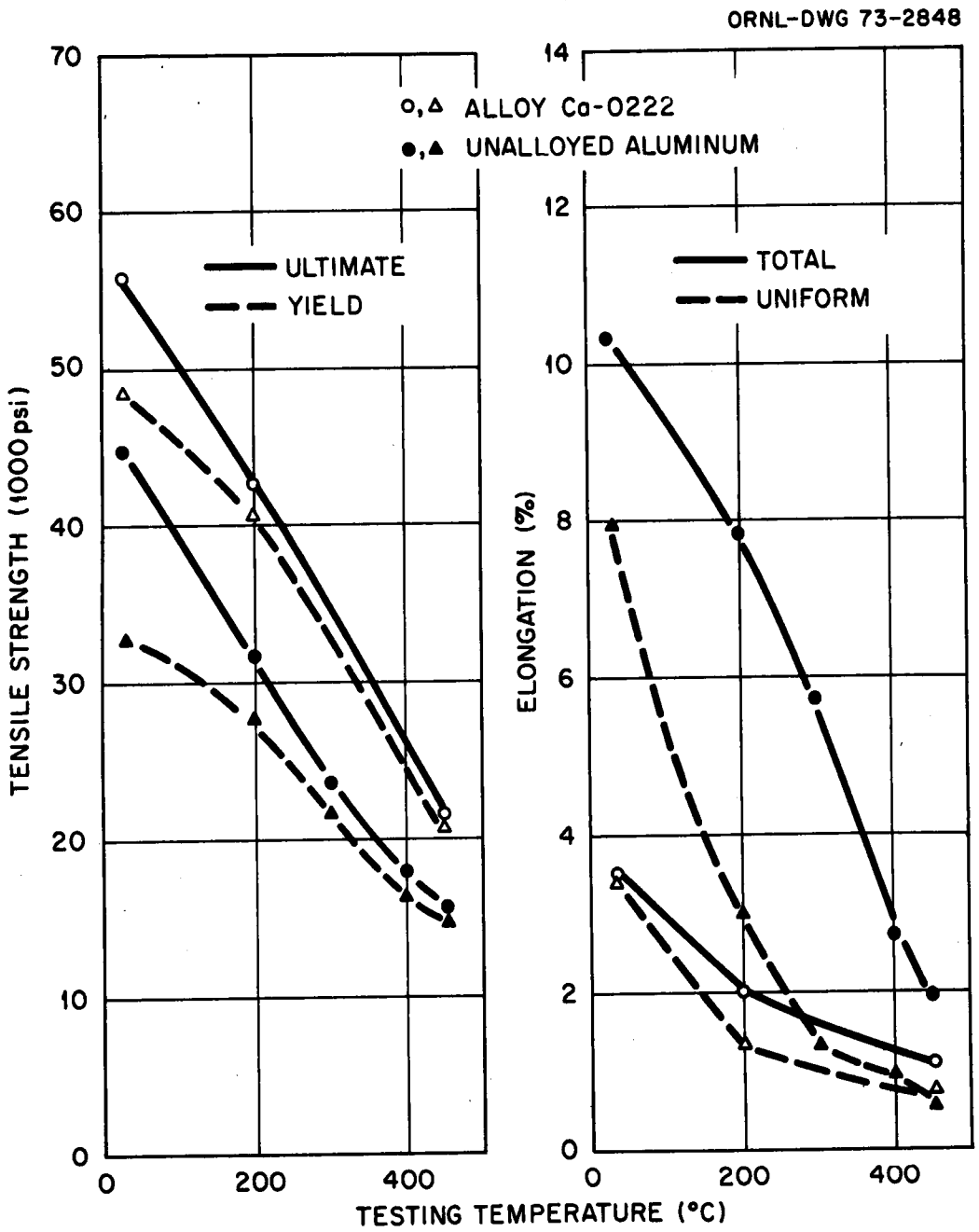

Figure 17. Tensile Properties of Experimental Alloyed and Unalloyed SAP as a Function of Testing Temperature. Ball-milled 10 hours.

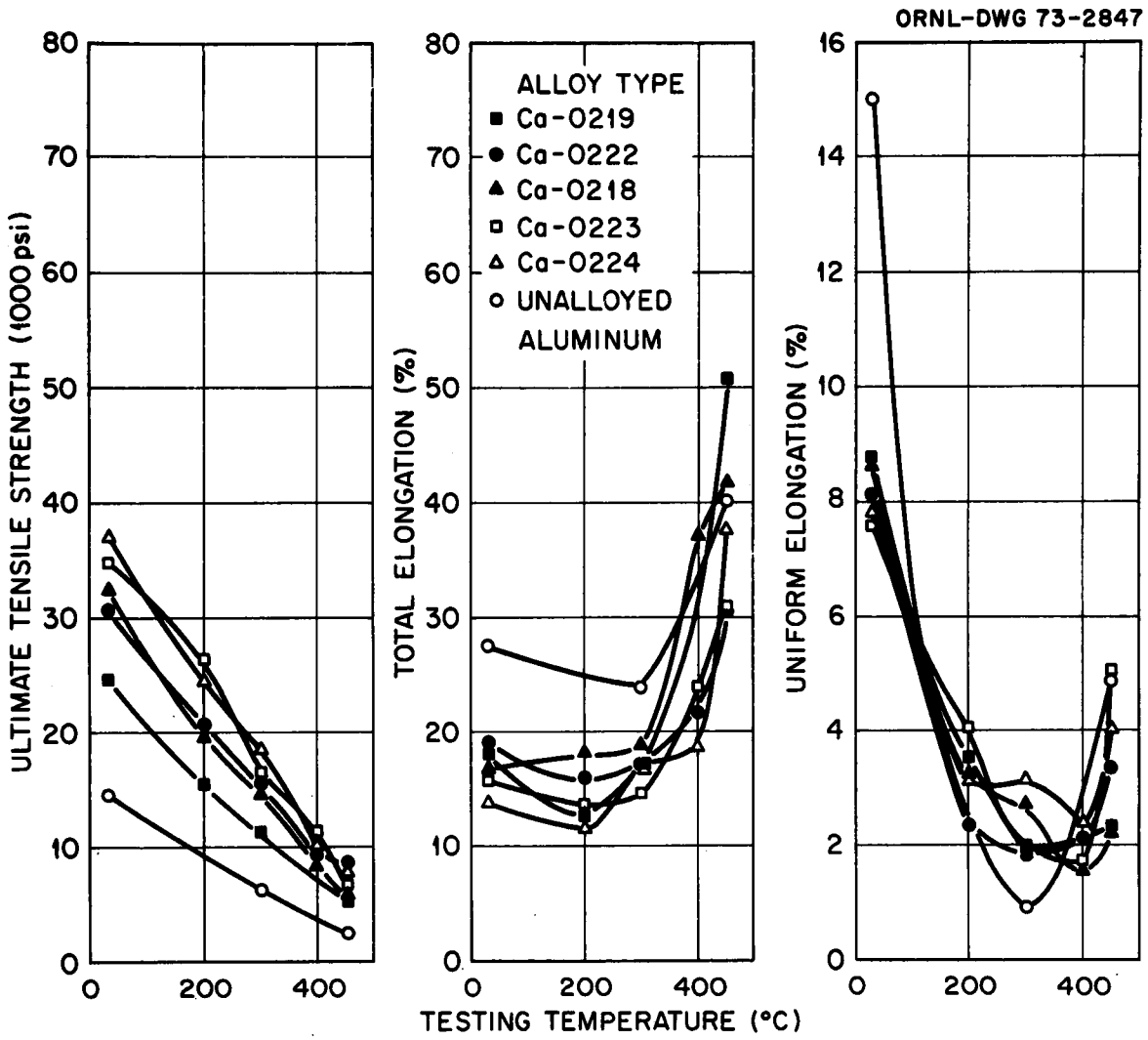

Figure 18. Tensile Properties of Experimental Alloys With No Ball-Milling as a Function of Testing Temperature.

The tensile properties of oxide dispersion-strengthened (10 hours ball-milling) unalloyed aluminum, 6% magnesium in aluminum, and alloy CA-0222 are compared to a conventional precipitation strengthed aluminum alloy 2219-T6 in Figure 19. Alloy 2219 contains 6.3% copper and was developed by Alcoa for elevated-temperature application. (39) As expected, the conventional alloy has inferior strength above about 275°C with much higher elongation at all temperature. The additional strengthening due to magnesium is especially effective below 200°C. The strength increase due to the intermetallic compounds is almost a constant additive to the oxide dispersion strengthening at all testing temperatures. The tensile data for all the alloys investigated are tabulated in the appendix.

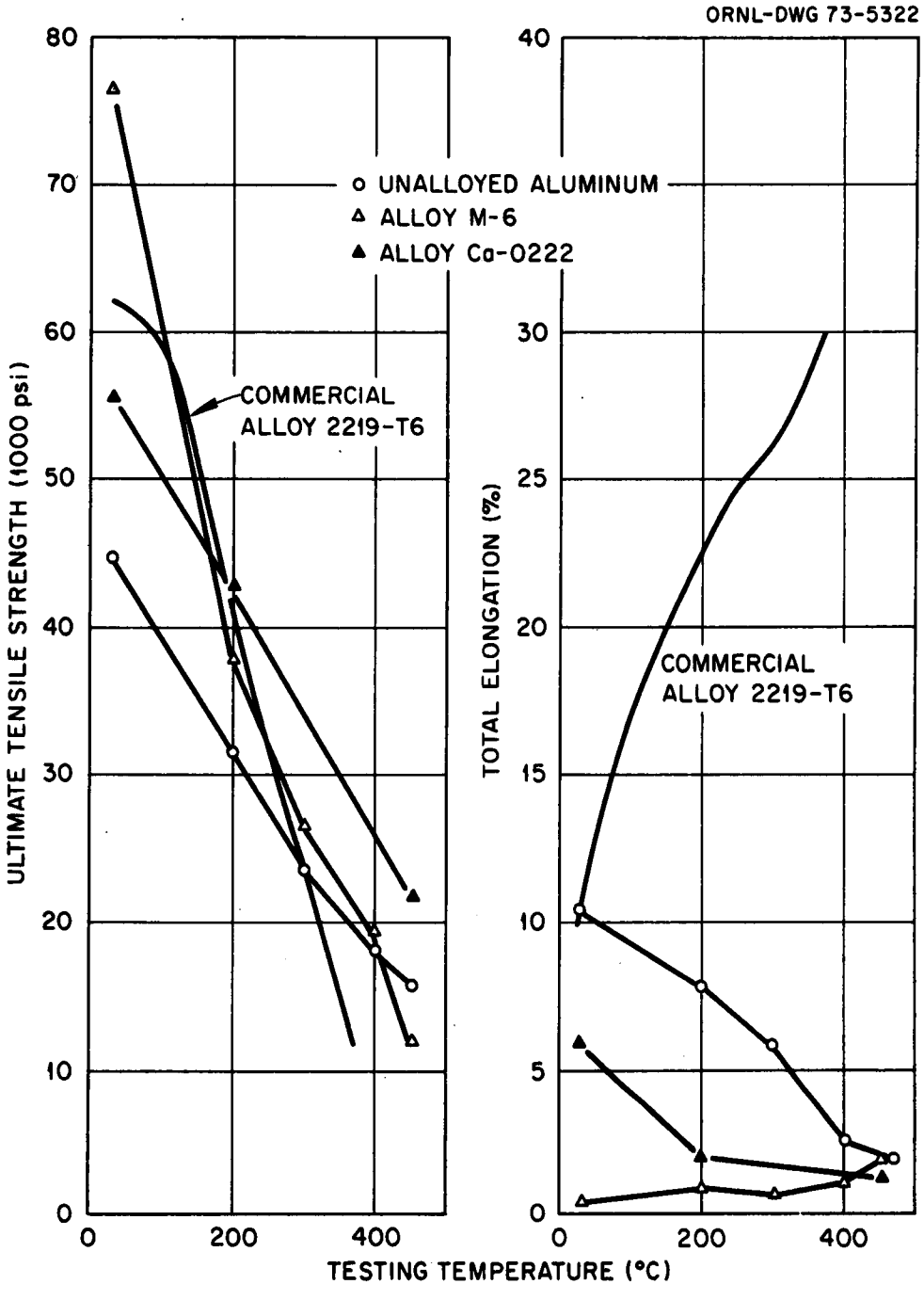

Figure 19. Tensile Properties of Experimental Alloys with 10 Hours Ball-Milling and a Commercial Alloy as a Function of Testing Temperature.

CHAPTER VII

DISCUSSION OF FRACTURE MECHANISM

Typical examples of the fracture surfaces of tensile samples of these alloys as shown by scanning electron microscopy are presented in Figures 20 through 25. These examples show both types of alloys and unalloyed aluminum at two levels of oxide content after testing at 450°C. Comparison of the alloys to unalloyed SAP and to previous results by Harman and Nolan (21,22) shows that the fracture mechanism is unchanged by the addition of these alloying elements.

Fracture first begins as void formation at large oxide agglomerates or stringers and as strain progresses, voids form on smaller particles. These voids can subsequently grow and coalesce to form cracks and fissures throughout the material. The resultant stress concentration and uneven loading leads to a tearing fracture mode in which the fracture advances from void to void with great local deformation. As the separation and tearing decreases the area and raises the stress level, final failure is by shear. This process is illustrated schematically in Figure 26. The relative importance of these fracture modes depends primarily on temperature and secondarily on strain rate. At high temperatures, separation and tearing predominate with only minor shear. At low temperatures, shear predominates. Increasing strain rate tends to increase the amount of shear fracture and the measured elongation.

Harman and Nolan (22) have determined the amount of voiding as a function of strain at 450°C by prestraining samples at 450°C, then tensile testing to fracture at −196°C. The voids and fracture features

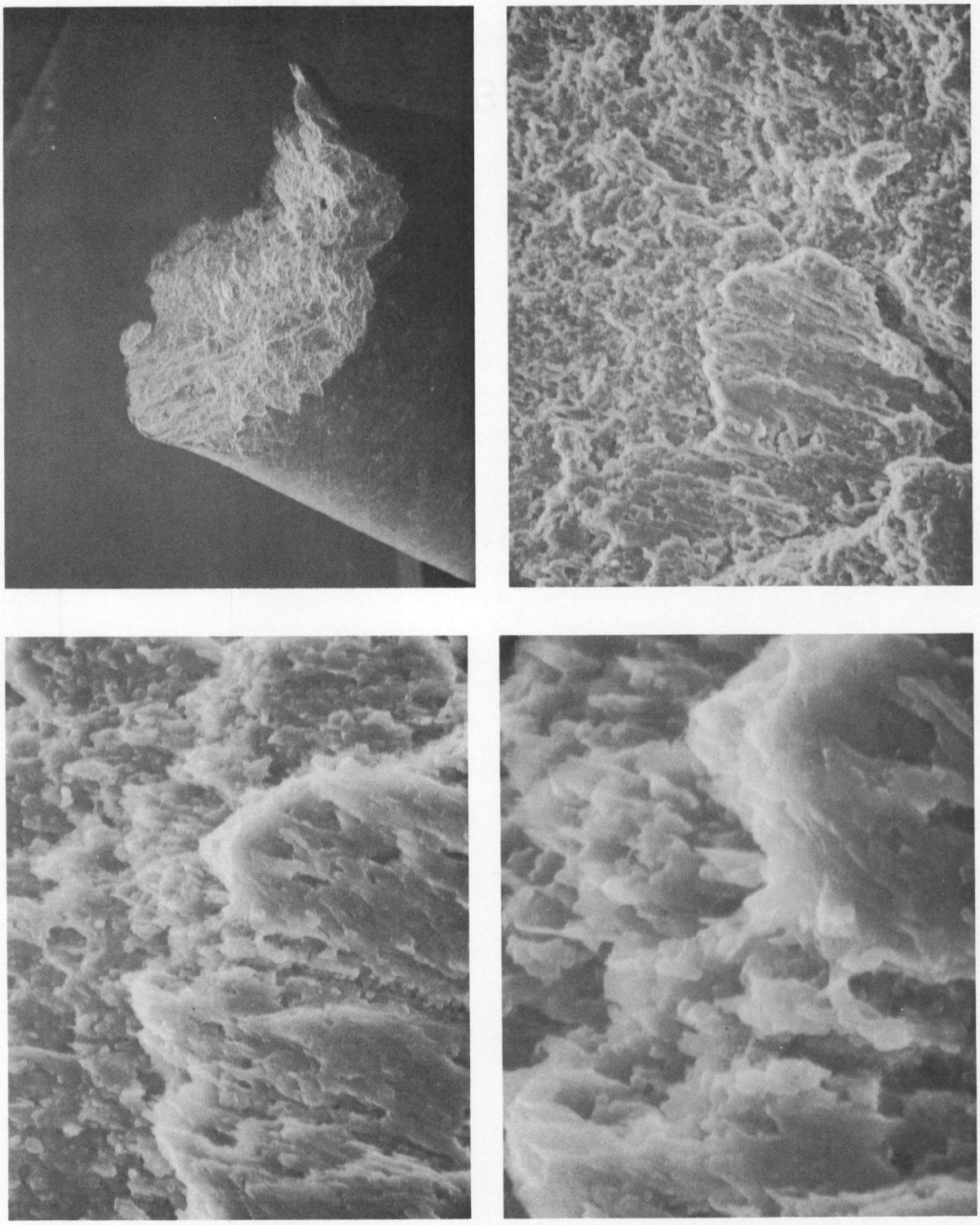

Figure 20. Scanning Electron Micrographs of Fracture Surface of Experimental Unalloyed SAP with 2 Hours Ball-Milling. Magnifications are top left 50x, top right 500x, lower left 2000x, and lower right 5000x.

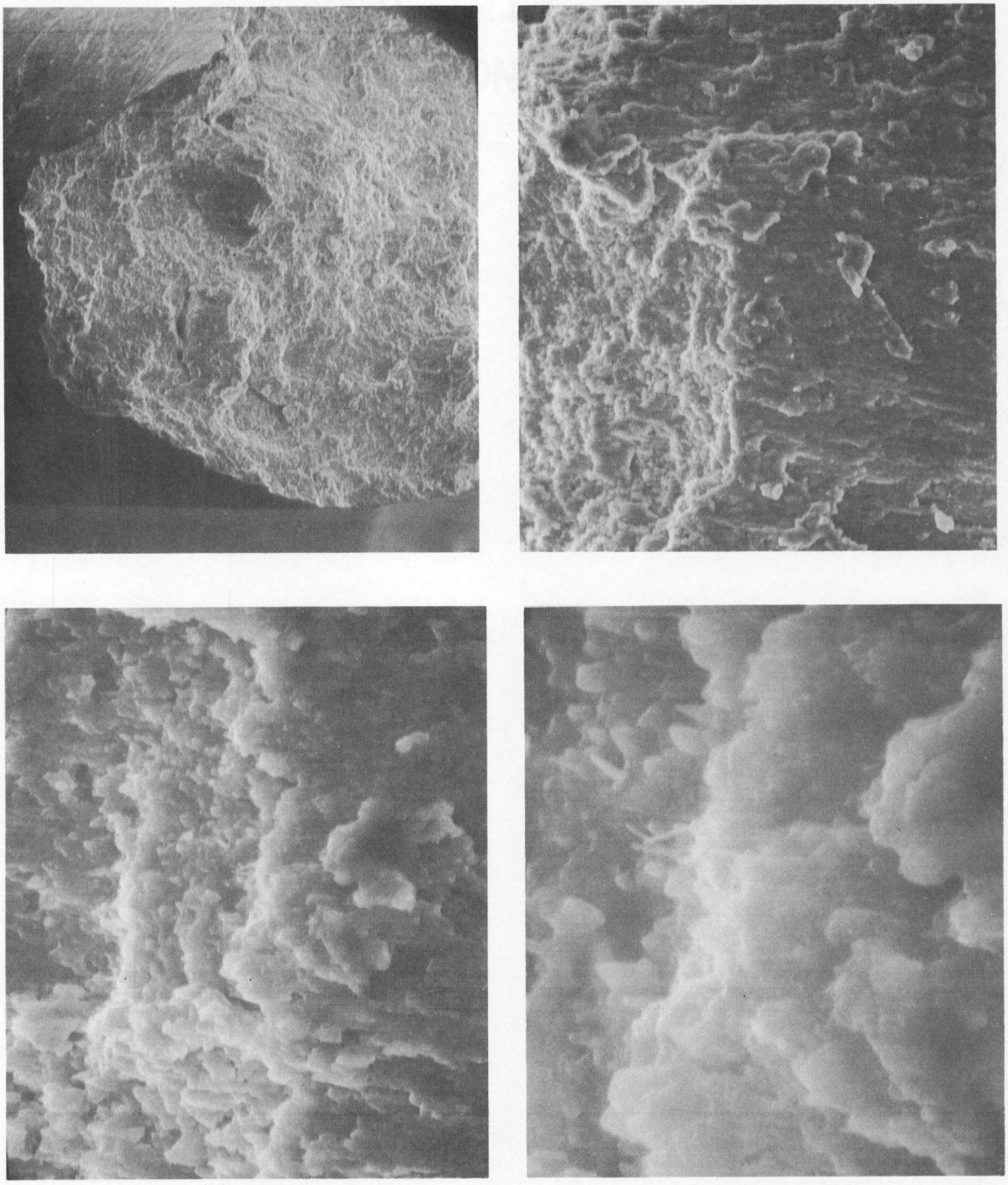

Figure 21. Scanning Electron Micrographs of Fracture Surface of Alloy M-6 With 2 Hours Ball-Milling. Magnifications are top left 50x, top right 500x, lower left 2000x, and lower right 5000x.

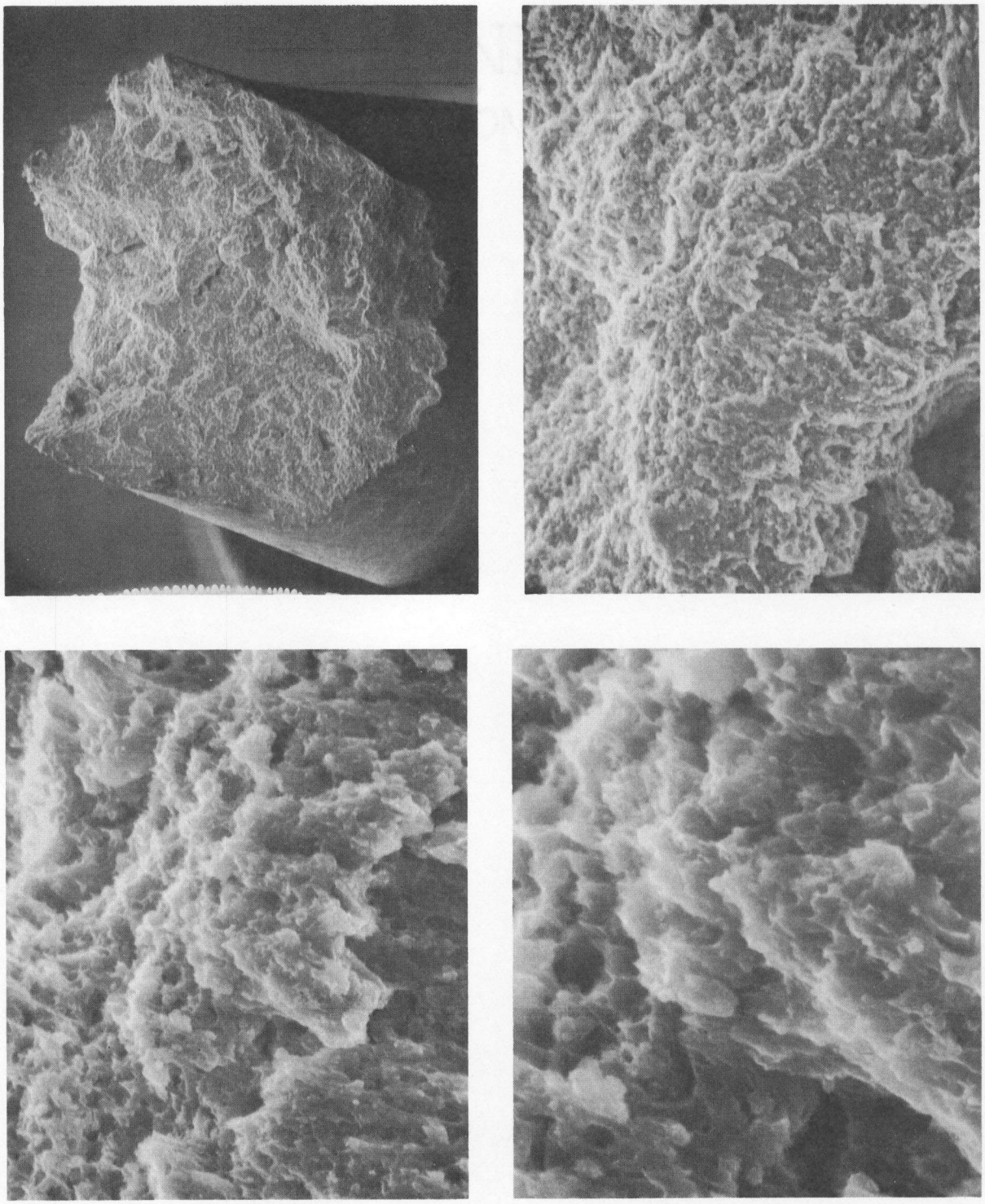

Figure 22. Scanning Electron Micrographs of Fracture Surface of Alloy CA-0223 With 2 Hours Ball-Milling. Magnifications are top left 50x, top right 500x, lower left 2000x, and lower right 5000x.

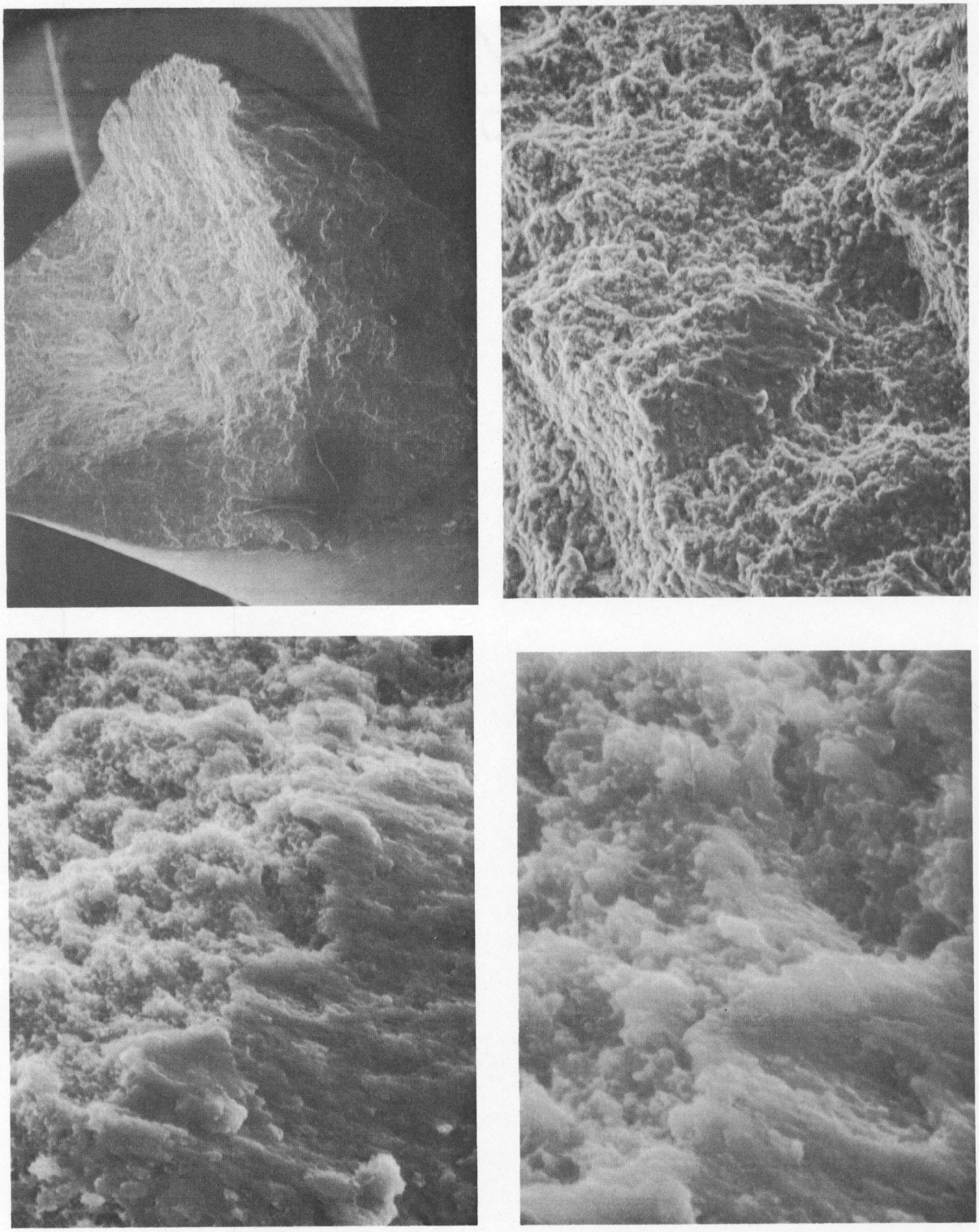

Fig. 23. Scanning Electron Micrographs of Fracture Surface of Alloy M-6 With 10 Hours Ball-Milling. Modifications are top left 50x, top right 500x, lower left 2000x, and lower right 5000x.

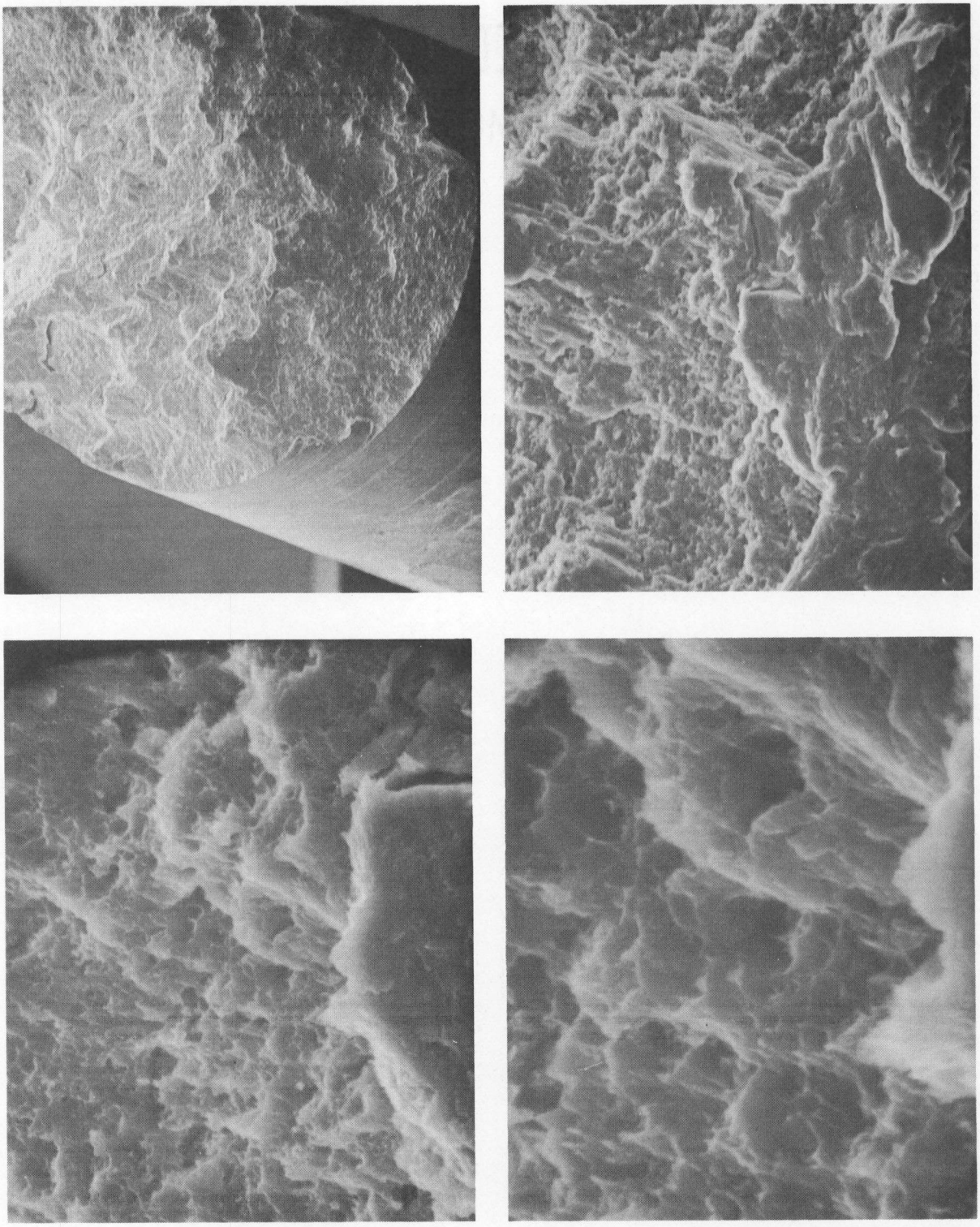

Figure 24. Scanning Electron Micrographs of Fracture Surface of Experimental Unalloyed SAP With 8 Hours Ball-Milling. Magnifications are top left 50X, top right 500X, lower left 2000X, and lower right 5000X.

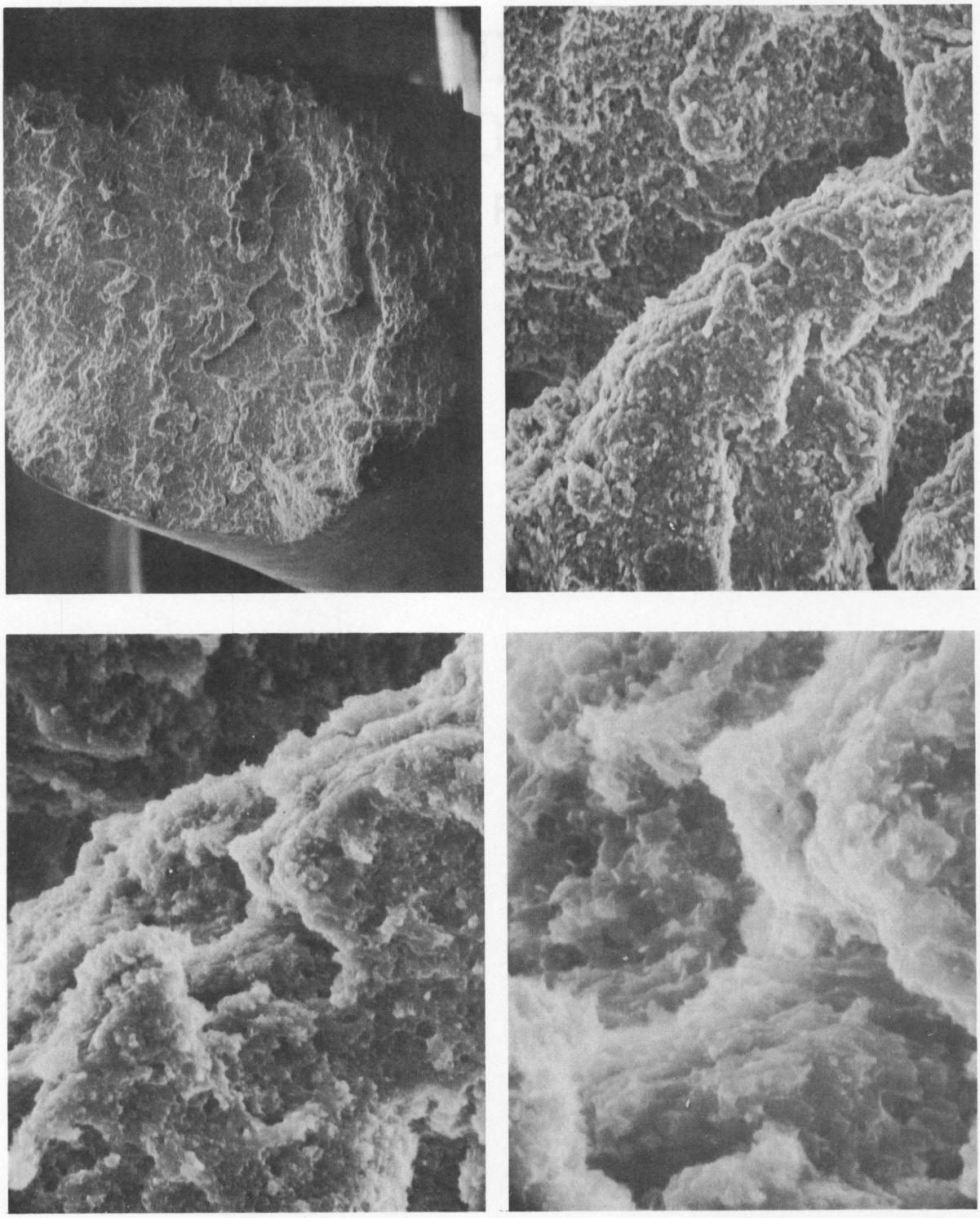

Figure 25. Scanning Electron Micrographs of Fracture Surface of Alloy CA-0223 With 10 Hours Ball-Milling. Magnifications are top left 50x, top right 500x, lower left 2000x, and lower right 5000x.

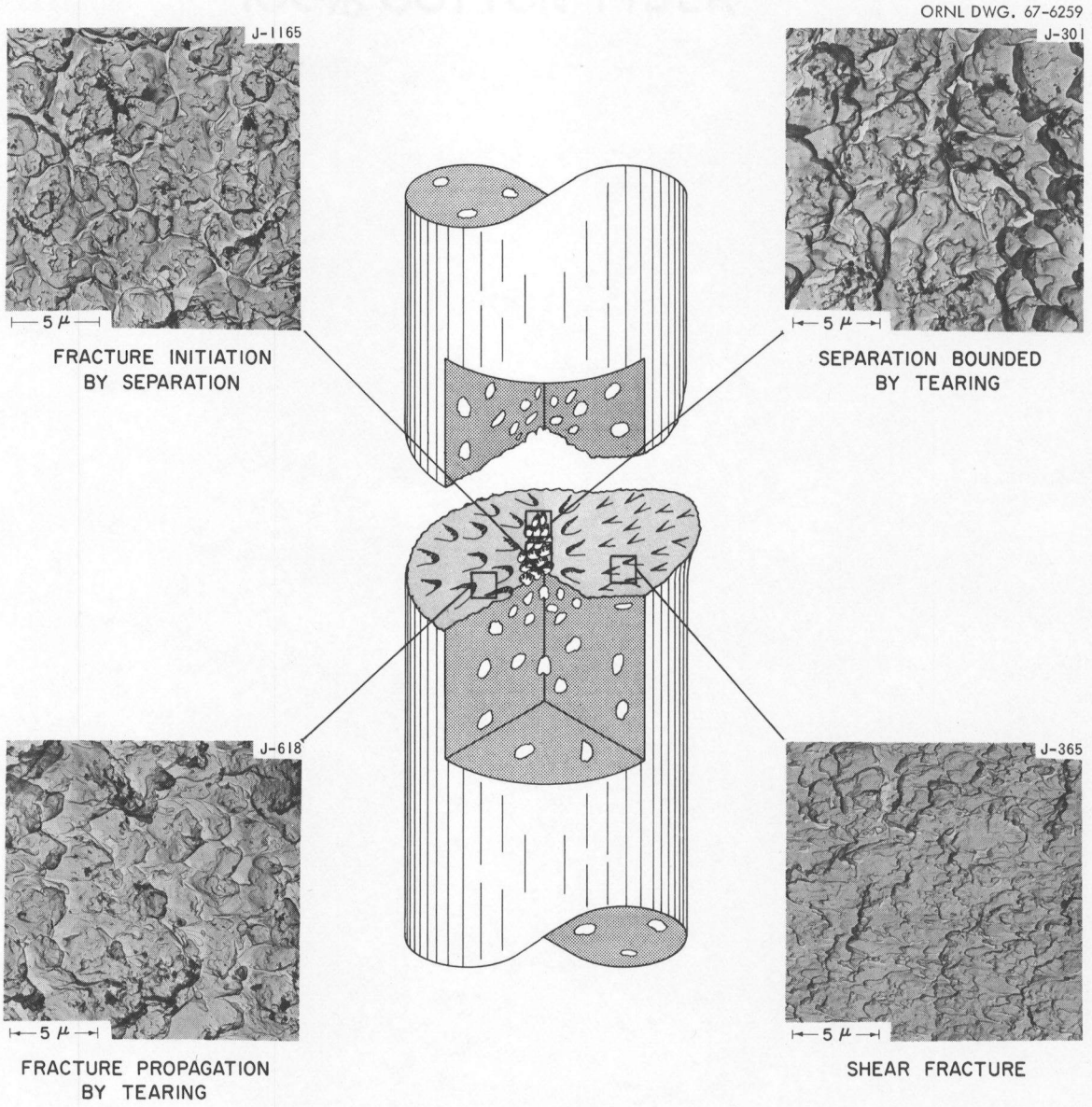

Figure 26. Typical Features Observed After Fracture of Unalloyed SAP at High Temperature. From Harman and Nolan (reference 21).

formed at 450°C are readily distinguished from those formed at −196°C due to their large size. Both the number density and size of the voids formed at 450°C increased with the amount of strain. As would be expected, the tensile strength of the samples as tested at −196°C decreased with increasing prestrain at 450°C as shown in Figure 27. The decrease was linear with measured void area formed at 450°C as shown in Figure 28. This result indicates that although the strengthening mechanism of SAP-type alloys may not be changed by high-temperature exposure, the post-heating strength will be reduced due to void formation if the alloy is strained at high temperature.

Kellerer and Piatti (40) have also observed the correlation of void volume with strain at 450°C by density decreases in strained samples. They observed greater decreases in density with slower strain rates. They also introduced large amounts of strain in samples by swaging at room temperature. This deformation resulted in density decreases due to void formation around the second-phase particles. Strength and ductility decreases are usually observed after cold working of SAP alloys and these have been generally attributed to "microcracks" forming at the particle-matrix interface. (23) Gualandi et al. (5) have observed a correlation of decreased elongation at both high and low testing temperatures with increased frequency of microcracks.

Ashby (41) has proposed a model which accounts for the void or microcrack formation in the particle-matrix interface. An applied stress (either tensile or compressive) results in a tensile stress on the particle-matrix interface. It is difficult to calculate the magnitude of the tensile stress, but it can be shown to increase in an approximately

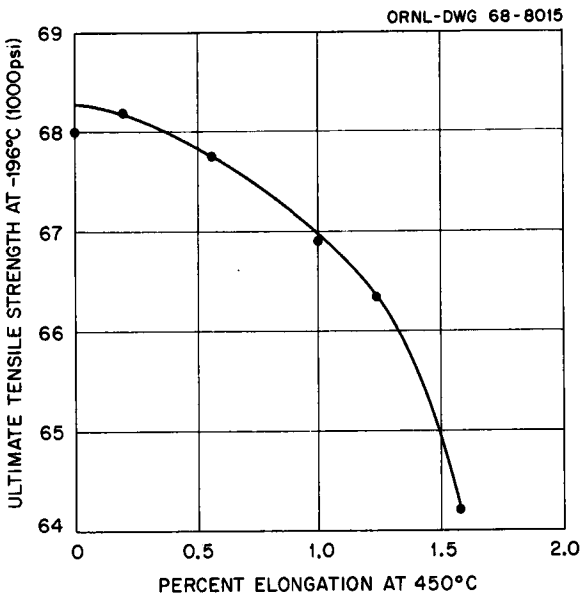

Figure 27. Tensile Strength of Unalloyed SAP at −196°C as a Function of Prior Prestrain at 450°C. From Harman and Nolan. (22)

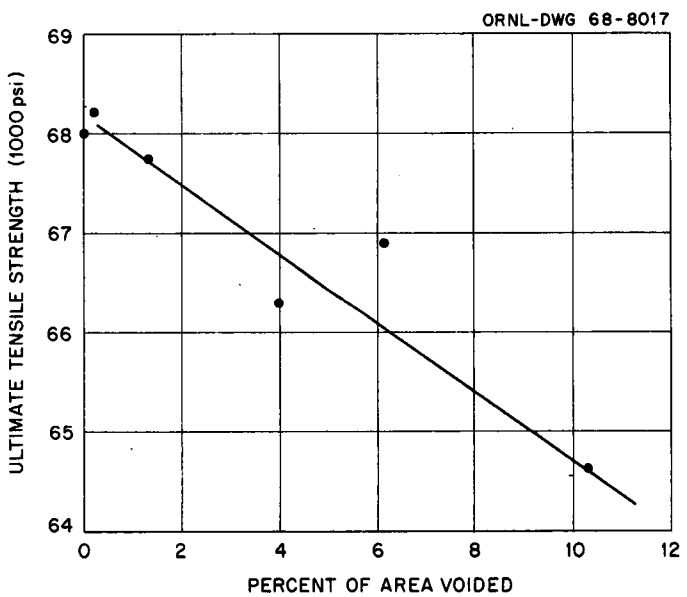

Figure 28. Tensile Strength of Unalloyed SAP at −196°C as a Function of the Amount of Cross-Sectional Area Lost Due to Voiding During Prestrain. From Harman and Nolan. (22)

linear fashion with strain and particle diameter. When the stress exceeds the tensile strength of the particle-matrix interface, cavitation will occur. Further calculations show that once cavitation occurs, the volume of a cavity will increase linearly with strain. Also with increasing strain, cavities will begin to form on smaller dispersed particles. Experimental evidence such as presented by Harman and Nolan (22) and Kellerer and Piatti (40) shows that void formation in SAP-type alloys begins essentially as soon as any strain occurs during tensile testing at 450°C. Voids occur first at agglomerations or stringers of oxide particles which may behave as very large particles.

Schiller and Schneiders (42) have reported an experiment which further supports the model of Ashby. They report increased elongation values for SAP-type alloys prepared with a uniform dispersion of much smaller particles than ordinarily found in SAP. A long-term high-temperature treatment which caused the particle size to increase resulted in lower elongation values.

The fact that the intermetallic compounds do not effect the fracture appearance or uniform elongation may at first seem surprising in view of their size as compared to the oxide particles. The relative sizes of the individual oxide particles and intermetallic particles are shown in the transmission electron micrographs in Figures 29 through 33. The oxide particles are typically disk-shaped with thicknesses about 0.02 μm. The intermetallic compounds are typically equiaxed about 0.25 to 0.5 μm diameter. However, the larger agglomerates of oxides do not show up in transmission electron microscopy due to the difficulty of uniformly thinning these areas. It is probable that the large oxide agglomerates

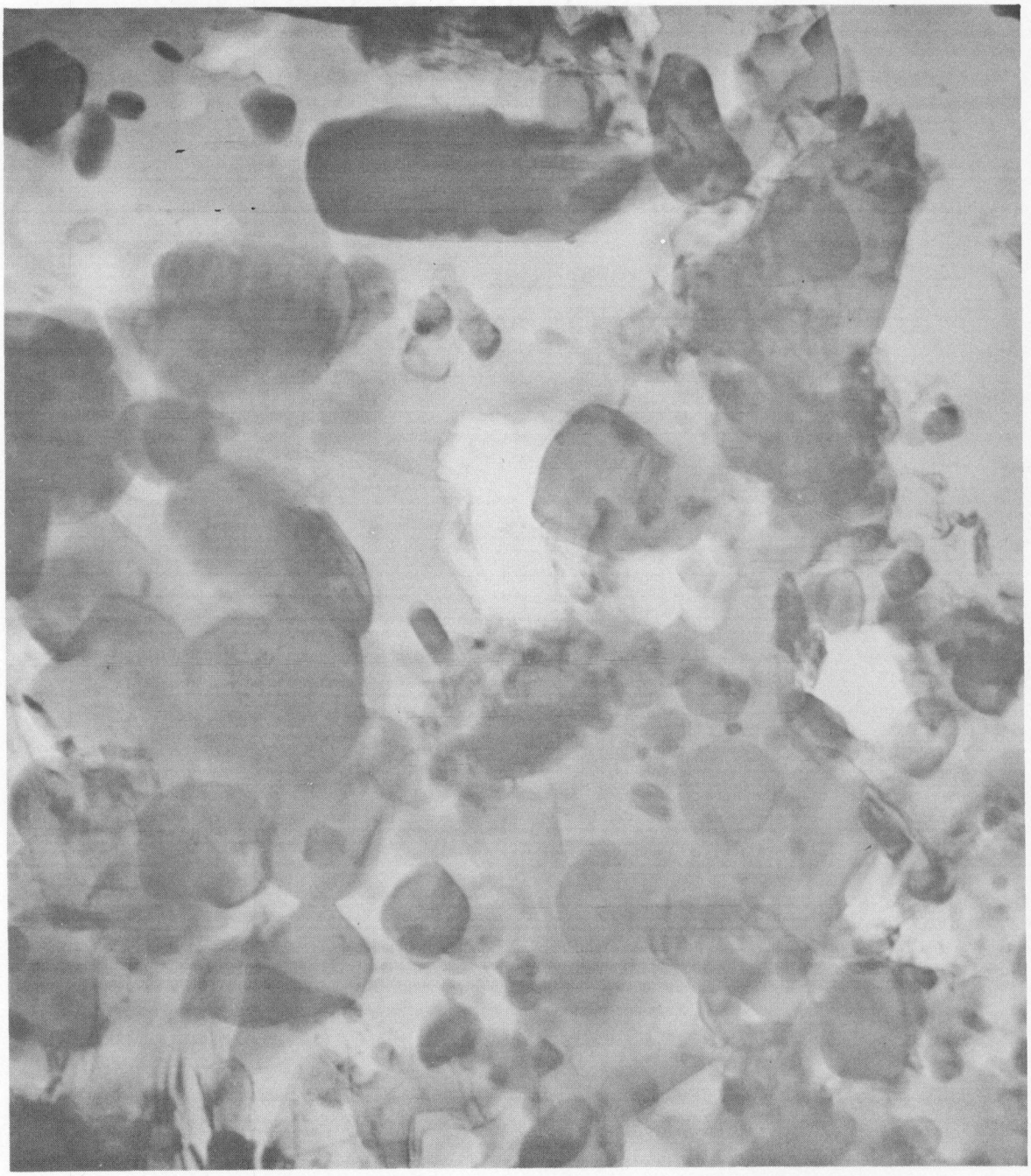

Figure 29. Transmission Electron Micrograph of Alloy CA-0223 with No Ball-Milling. (50,000x)



Figure 30. Transmission Electron Micrograph of Alloy CA-0223 with 2 Hours Ball-Milling. (50,000X)

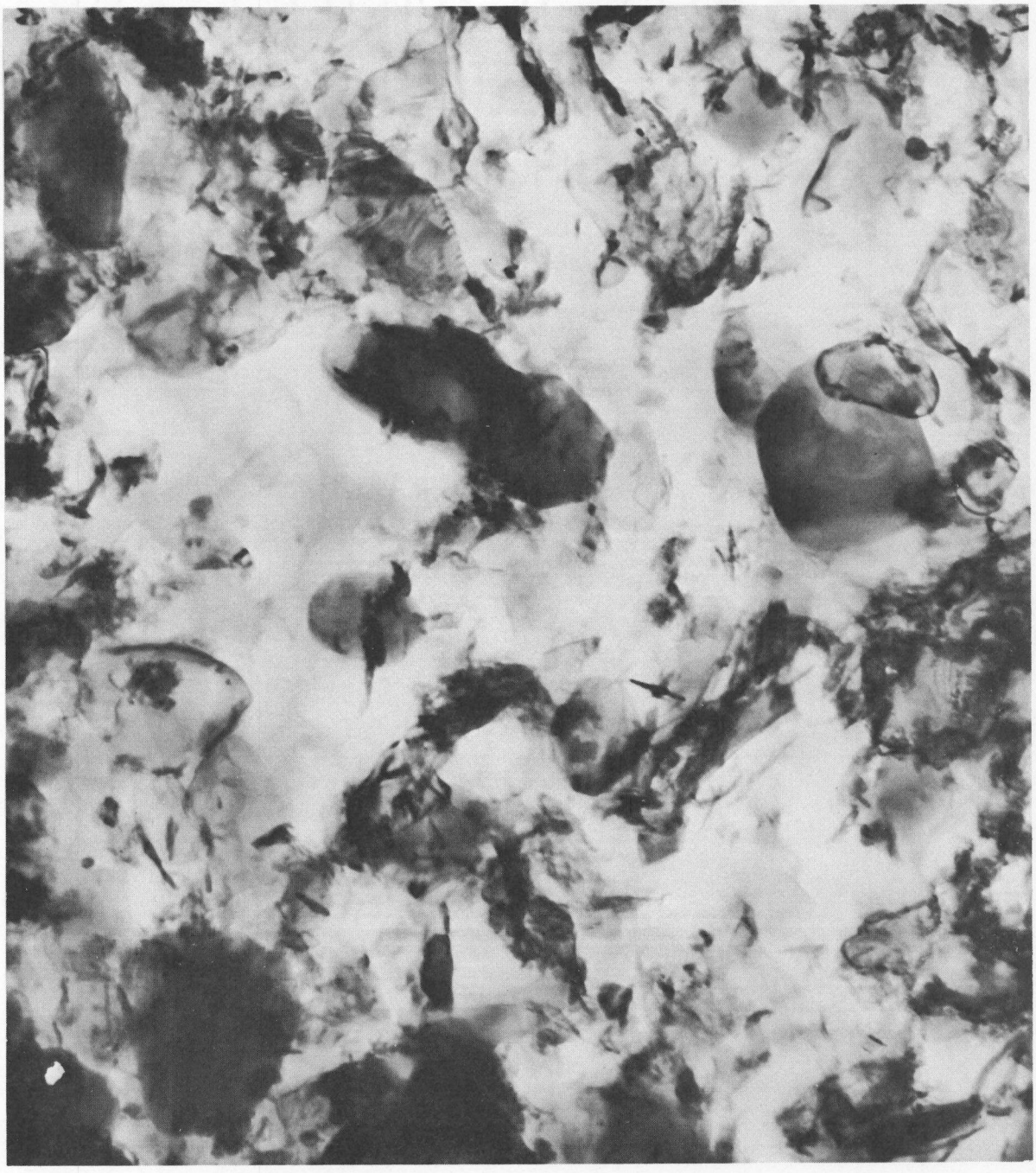

Figure 31. Transmission Electron Micrograph of Alloy CA-0223 with 8 Hours Ball-Milling. (50,000x)

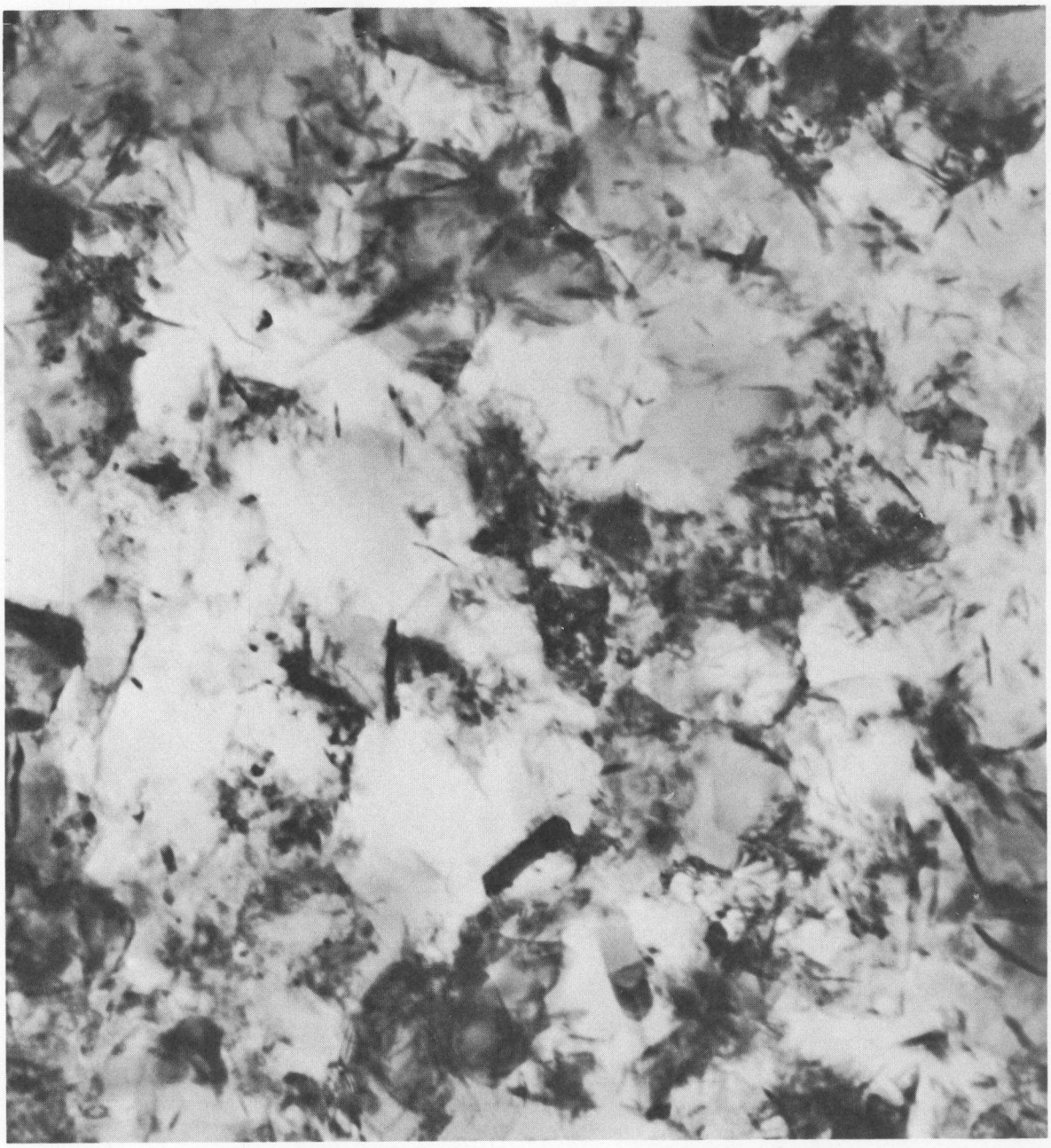

Figure 32. Transmission Electron Micrograph of Alloy CA-0223 with 10 Hours Ball-Milling. (50,000x)



Figure 33. Transmission Electron Micrograph of Alloy CA-0223 with 10 Hours Ball-Milling. (100,000X)

control the initiation of fracture. Another factor could be the possibility of a stronger interface between the intermetallics and the matrix resulting in void formation at about the same strain levels as when the intermetallics are not present. Investigation of this possibility is beyond the scope of this work but could provide an area of further research.

Comparison of the intermetallic compound sizes in Figures 31 through 33 illustrates the effectiveness of the finely distributed oxide in preventing growth of the intermetallic compounds at high temperatures. All four of the alloys have had the same thermal history of 20 hours at 600°C plus about 1 hour at 500°C. The intermetallic particles in Figure 29 (powder not ball-milled) are considerably larger than those in Figures 30, 31, and 32 for which the powders were ball-milled 2, 8, and 10 hours, respectively.

CHAPTER VIII

DISCUSSION OF STRENGTHENING MECHANISMS

Although the objective of this study was not to investigate the strengthening mechanisms of dispersion alloys, several observations may be made. The solid solution strengthening due to magnesium is additive to the strengthening from the oxide dispersion. This might imply that strengthening of unalloyed dispersions even at room temperature is due more to direct particle-dislocation interactions rather than buildup of forests and tangles from indirect particle-dislocation interactions. Otherwise, the high oxide content dispersions would tend to become saturated with tangles and forests so that the addition of magnesium would have little effect. The strengthening due to intermetallic compounds is additive to the oxide dispersion strengthening at all temperatures tested. The effects are greater at lower oxide contents and lower temperatures. These data are not in conflict with the mechanisms involving direct particle-dislocation interactions such as climb and cross-slip or shearing of particles.

Guyot (43) has attempted to correlate activation energies and microstructure as observed by transmission electron microscopy to determine the strengthening mechanisms in SAP. He concludes that at temperatures below about −100°C, forest mechanisms control plastic flow. In the region from about −100°C to 100°C he suggests that the particles interact directly with dislocations as well as have an indirect effect by acting

as sources for creating additional dislocations. He concludes that deformation is controlled by cross-slip between 100 and 200°C and by climb of dislocations between 200 and 300°C. Above 350°C the high activation energies do not correlate with any single identifiable mechanism for deformation.

CHAPTER IX

CONCLUSIONS

Based on this investigation the following conclusions and observations are offered from the fabrication process development on unalloyed aluminum.

1. Mechanical testing conditions, especially strain rate and temperature, significantly affect properties. The testing conditions must be known and accurately controlled for meaningful comparisons.

2. The developed process yields uniform and consistent material with strengths greater than that of commercially available SAP 895. The critical processing steps are ball-milling of flake powder to a reproducible oxide content and conversion of the hydrated oxide to a stable form.

3. The higher strength of the experimental material over SAP 895 is a result of improved distribution of the oxide. It is suggested that elimination of agglomeration and welding of particles during ball-milling is responsible for the improved oxide distribution.

4. Increases in oxide content that occur after ball-milling have little if any effect on strength of extruded material.

5. Hydrogen contents greater than approximately 5 ppm result in degradation of tensile strength, blistering, or both in SAP rod during exposure to air at 600°C for 40 hours.

6. Inclusions of iron up to 3% or Al_4C_3 resulting from carbon up to 2% has no significant effect on either the magnitude of the as-extruded tensile strength or the thermal stability of SAP rods.

This investigation has shown that potentially useful improvements can be made in oxide dispersion-strengthened aluminum by producing them from prealloyed aluminum powder. The following specific conclusions and observations are offered.

1. Magnesium additions provide additional strength up to 200°C with very little decrease in 450°C properties. SAP alloys with room temperature strengths of 77,000 psi were produced with 6% magnesium additions.

2. Additions of elements which form insoluble intermetallic compounds in aluminum provide additional dispersion strengthening when produced by atomizing. This additional strengthening is additive to the oxide dispersion strengthening from room temperature to 450°C.

3. Uniform elongation of the oxide dispersion-strengthened alloys is low at elevated temperatures even at very low oxide contents so that no significant improvement in ductility results from lower oxide content.

4. The alloys produced from the atomized powders containing insoluble intermetallic compounds with no ball-milling possess good strengths (about half that of a typical SAP) at 450°C with much higher elongations than SAP.

5. Failure is initiated by cavity formation at the oxide particles (or oxide agglomerates) matrix interface. Cavity formation and growth continue in a localized plane until final failure occurs by shear as the stress builds up due to the decrease in area.

6. The room temperature strengths of both the magnesium and intermetallic compound alloys will not be affected by exposure to temperatures up to 450°C unless the exposure is accompanied by strain and resultant cavity formation.

7. The data tend to suggest the theories of direct particle-dislocation interactions as the dominant strengthening mechanisms in dispersion strengthened aluminum.

LIST OF REFERENCES

LIST OF REFERENCES

1. R. Irmann, Metallurgia, Sept. 1952, p. 125.

2. Mena G. Andrews, SAP for Heavy Water Organic Cooled Reactors, Atomics International–Combustion Engineering Joint Report, Feb. 13, 1967.

3. Euratom Scientific Activities ORGEL Program: Theoretical and Conceptual Studies, Euratom Report EUR 1830e (1964).

4. G. L. Copeland, M. M. Martin, D. G. Harman, and W. R. Martin, Effect of Powder and Process Variables on the Properties of Sintered Aluminum Products, Oak Ridge National Laboratory Report ORNL-TM-2215 (May 1968).

5. D. Gualandi, et al., Dispersion Strengthened Aluminum for Nuclear Purposes, With Particular Emphasis on Correlation Between Strength and Microstructure Parameters, Euratom Report EUR-4035e (1968).

6. R. J. Towner, Metals Enginering Quarterly, 6, Feb. 1961, p. 24.

7. Albert G. Guy, Elements of Physical Metallurgy, Addison-Wesley, Reading, Mass., 1960.

8. A. H. Cottrell, Dislocation and Plastic Flow in Crystals, Claredon Press, Oxford, 1953.

9. R. F. Bunshah and C. G. Goetzel, A Survey of Dispersion Strengthening of Metals and Alloys, Wright-Patterson Air Force Base Report WADC-TR-59-414 (March 1960).

10. G. S. Ansell, "The Mechanism of Dispersion Strengthening; A Review," p. 61 in Oxide Dispersion Strengthening (G. S. Ansell, T. D. Cooper, and F. V. Lenel, Eds.), Gordon and Breach, New York, 1968.

11. E. Orowan, Discussion of paper by Sir Lawrence Bragg, "Effects Associated with Stresses on a Microscopic Scale," in Symposium on Internal Stresses in Metals and Alloys, Institute of Metals, London, 1948.

12. M. F. Ashby, Electron Microscopy and Strength of Crystals, Interscience, New York, 1963, p. 891.

13. A. Kelly and R. B. Nicholson, Progress in Materials Science, 10, No. 3 (1963).

14. G. S. Ansell and F. V. Lenel, Acta Met., 8 (1960), p. 612.

15. N. F. Mott and F.R.N. Nabarro, Proc. Phys. Soc., 52 (1940), p. 86.

16. D. Dew-Hughes, Acta Met., 8 (1960), p. 816.

17. N. J. Grant and O. Preston, Trans. AIME, 209 (1957), p. 349.

18. N. J. Grant and O. Preston, Trans. AIME, 221 (1961), p. 164.

19. P. Guyot, "On the Mechanisms of Plastic Deformation of SAP-Type Alloys," Modern Developments in Powder Metallurgy, Vol. 3 (H. H. Hausner, Ed.), Plenum Press, New York, 1966.

20. R. W. Frazer, B. Meddings, D.J.I. Evans, and D. J. Mack, Modern Development in Powder Metallurgy, Vol. 3, (H. H. Hausner, Ed.), Plenum Press, New York, 1966.

21. D. G. Harman and T. A. Nolan, Fracture of Al–Al_2O_3 Alloys: Fracture Analysis of the Commercial SAP-Type Alloy XAP-001, Oak Ridge National Laboratory Report ORNL-TM-1826, July 1967.

22. D. G. Harman and T. A. Nolan, Fracture Initiation in XAP-001 SAP Alloy, Oak Ridge National Laboratory Report ORNL-TM-2324, Feb. 1969.

23. D. Gualande and P. Jehenson, "Powder Metallurgy of Al–Al_2O_3 Composites (SAP) for Nuclear Applications," Modern Developments in Powder Metallurgy, Vol. 3, (H. H. Hausner, Ed.), Plenum Press, New York, 1966.

24. D. G. Harman, Mechanical Properties of Al–Al_2O_3 Alloys: Testing Procedures and Evaluation of Data, Oak Ridge National Laboratory Report ORNL-TM-1802, May 1967.

25. Kent R. Van Horn, Ed., Aluminum, Vol. I: Properties, Physical Metallurgy, and Phase Diagrams, American Society for Metals, Metals Park, Ohio, 1967.

26. Max Hansen, Constitution of Binary Alloys, McGraw-Hill, New York, 1958.

27. F. A. Shunk, Constitution of Binary Alloys, Second Supplement, McGraw-Hill, New York, 1969.

28. R. P. Elliott, Constitution of Binary Alloys, First Supplement, McGraw-Hill, New York, 1965.

29. R. Irmann, Paper presented at Congres International de l' Aluminum, VI, Paris, June 14–19, 1954, Malescherbes, Paris, 1955.

30. G. Ito and F. Sawayonagi, Rept. Sci. Research Inst., Tokyo, 34 (1958), p. 266.

31. I. N. Fridlyander and B. I. Matveyev, Eds, A High Temperature Material Made of Sintered Aluminum Powder (SAP), Translation JPRS 17, 818.

32. A. S. Bufferd and N. J. Grant, Trans. ASM, 60 (1967), p. 305.

33. Niels Hansen, Trans. TMS-AIME, 242 (May 1968), p. 954.

34. J. Herenguel and J. Boghen, "Properties des demi-products in Aluminum Fritté," Congres International de l' Aluminum, VI, Paris, June 14-19, 1954, Malescherbes, Paris, 1955, p. 341.

35. Karl Wefers and Gordon M. Bell, Oxides and Hydroxides of Aluminum, Alcoa Research Laboratories Technical Paper No. 19, 1972.

36. N. Hansen and E. Adolph, The Effect of Heat Treatment on the Structural Stability of Aluminum Products, Danish Atomic Energy Research Establishment, Risö Report 25, May 1961.

37. N. Hansen, Powder Metallurgy, 10 (1967) No. 20, p. 94.

38. C.K.H. DuBose and J. O. Stiegler, Semiautomatic Preparation of Specimens for Transmission Electron Microscopy, Oak Ridge National Laboratory Report ORNL-4066 (Feb. 1967).

39. L. W. Mayer, Alcoa Aluminum Alloy 2219, Aluminum Company of America Green Letter, Oct. 1, 1960.

40. H. Kellerer and G. Piatti, J. Materials Science, 3 (1968), p. 486.

41. M. F. Ashby, "The Theory of the Critical Shear Stress and Work Hardening of Dispersion-Hardened Crystals," Oxide Dispersion Strengthening, (G. S. Ansell, T. D. Cooper, and F. V. Lenel, Eds.) Gordon and Breach, New York, 1968.

42. P. Schiller and A. Schneiders, J. Nucl. Matls., 27 (1968), p. 115.

43. P. Guyot, "On The Mechansisms of Deformation in Dispersion-Hardened Alloys," Oxide Dispersion Strengthening, (G. S. Ansell, T. D. Cooper, and F. V. Lenel, Eds.) Gordon and Breach, New York, 1968.

APPENDIX

TABLE 13

TENSILE PROPERTIES OF DISPERSION STRENGTHENED UNALLOYED ALUMINUM

Sample No.	Ball-Milling Time (hr)	Test Temperature (°C)	Elongation (%)		Tensile Strength (psi)	
			Uniform	Total	Yield	Ultimate
MD-101-A-8	None	27	15.1	27.5	11,100	14,700
-10	None	300	0.84	23.7	5,740	6,090
-9	None	450	4.75	40.0	2,280	2,590
MD-101-2-5	2	27	7.63	13.94	19,984	25,775
-3	2	200	3.09	17.56	13,458	16,476
-2	2	300	1.18	11.2	11,623	12,031
-4	2	400	0.57	4.75	8,687	8,786
-1	2	450	0.49	4.05	6,000	6,044
MD-101-8-6	8	27	7.97	11.2	32,600	43,700
-7	8	200	3.10	8.22	26,274	29,936
-10	8	300	1.50	4.13	20,600	23,000
-8	8	400	0.87	3.07	18,379	19,048
-5	8	450	0.73	2.12	15,300	16,100
MD-101-10-14	10	27	7.98	10.3	32,900	44,600
-6	10	200	2.96	7.76	27,962	31,596
-7	10	300	1.34	5.68	21,800	23,500
-13	10	400	0.91	2.51	16,156	17,896
-8	10	450	0.56	1.98	14,700	15,300
MD-101-12-8	12	27	5.97	5.97	38,500	51,200
-6	12	200	3.14	5.54	29.857	36,067
-5	12	300	1.48	5.15	23,900	25,600
-7	12	450	0.60	1.24	17,500	17,800

TABLE 14

TENSILE PROPERTIES OF DISPERSION STRENGTHENED ALUMINUM-2.0% MAGNESIUM ALLOYS

Sample No.	Ball-Milling Time (hr)	Test Temperature (°C)	Elongation (%)		Tensile Strength (psi)	
			Uniform	Total	Yield	Ultimate
M-7-A-9	None	27	11.0	16.6	17,800	32,200
-6	None	200	3.63	38.0	17,280	19,110
-5	None	300	0.73	53.8	9,750	9,910
-8	None	400	2.34	49.3	4,580	4,900
-10	None	450	4.32	68.7	3,170	3,710
M-7-2-5	2	27	5,20	6.98	27,280	27,750
-3	2	200	1.02	21.7	20,230	21,130
-2	2	300	0.60	15.2	12,240	12,480
-4	2	400	0.69	1.58	8,240	8,730
-1	2	450	0.77	5.2	5,840	6,130
M-7-8-6	8	27	4.20	7.49	41,200	46,400
-10	8	200	0.60	11.6	24,680	25,080
-9	8	300	0.34	10.1	14,500	14,600
-5	8	400	0.67	5.86	9,220	9,380
-8	8	450	0.63	6.54	6,970	7,150
M-7-10-5	10	27	4.20	6.60	44,900	49,000
-10	10	200	0.69	34.1	24,480	25,040
-8	10	300	0.31	7.26	15,620	15,700
-9	10	400	0.66	3.33	10,750	10,910
-7	10	450	0.99	13.4	7,060	7,300
M-7-12-9	12	27	0.97	5.49	47,900	49,000
-7	12	200	0.55	2.95	29,620	30,020
-6	12	300	0.56	1.09	21,000	21,300
-5	12	400	0.51	1.92	12,740	12,900
-8	12	450	1.00	4.63	8,990	9,310

TABLE 15

TENSILE PROPERTIES OF DISPERSION STRENGTHENED ALUMINUM-4.3% MAGNESIUM ALLOYS

Sample No.	Ball-Milling Time (hr)	Test Temperature (°C)	Elongation (%)		Tensile Strength (psi)	
			Uniform	Total	Yield	Ultimate
M-2-A-6	None	27	12.9	14.5	24,600	44,200
-9	None	200	4.28	51.2	22,130	24,120
-8	None	300	0.95	100.5	9,160	9,360
-5	None	400	3.42	75.7	3,500	4,220
-7	None	450	9.02	83.0	1,350	3,060
M-2-8-8	8	27	1.00	2.91	60,700	63,800
-6	8	200	0.56	10.8	30,490	30,810
-5	8	300	0.34	1.59	19,400	19,600
-4	8	400	0.39	1.88	13,220	13,300
-7	8	450	0.81	2.34	10,300	10,400
M-2-10-8	10	27	0.88	2.66	61,700	64,600
-9	10	200	0.55	6.25	31,040	31,600
-5	10	300	0.25	2.99	20,800	20,900
-6	10	400	0.33	2.11	14,330	14,410
-7	10	450	0.76	2.54	11,300	11,500
M-2-12-7	12	27	0.87	2.11	64,100	67,000
-5	12	200	0.54	1.16	32,380	33,330
-13	12	300	0.32	1.85	23,100	23,200
-8	12	450	0.48	1.12	12,600	12,800

TABLE 16

TENSILE PROPERTIES OF DISPERSION STRENGTHENED ALUMINUM-6.2% MAGNESIUM ALLOYS

Sample No.	Ball-Milling Time (hr)	Test Temperature (°C)	Elongation (%)		Tensile Strength (psi)	
			Uniform	Total	Yield	Ultimate
M-6-A-13	None	27	14.1	19.7	31,500	52,600
-12	None	200	0.22	44.8	23,570	24,440
-11	None	300	0.41	98.4	7,830	7,870
-9	None	450	9.92	50.2	2,530	2,770
M-6-2-5	2	27	5.88	6.24	37,450	52,860
-3	2	200	1.44	23.1	23,010	24,900
-2	2	300	0.50	35.6	9,510	9,590
-4	2	400	0.85	2.36	6,220	6,570
-1	2	450	0.69	2.20	6,150	6,400
M-6-8-8	8	27	0.80	0.80	75,000	77,200
-6	8	200	0.42	1.80	41,310	41,470
-7	8	300	0.34	0.77	28,800	30,000
-5	8	450	0	0.64	16,880	16,880
M-6-10-5	10	27	0.47	0.47	74,100	76,400
-7	10	200	0.40	2.27	37,560	37,960
-8	10	300	0.27	0.63	26,200	26,300
-10	10	400	0.33	0.90	19,000	19,080
-9	10	450	0.97	1.93	11,600	11,800
M-6-12-6	12	27	0.82	1.00	67,600	70,800
-9	12	300	0.33	2.20	20,300	20,460
-11	12	450	0.34	0.48	14,500	14,600

TABLE 17

TENSILE PROPERTIES OF DISPERSION STRENGTHENED ALLOY CA-0218[a]

Sample No.	Ball-Milling Time (hr)	Test Temperature (°C)	Elongation (%)		Tensile Strength (psi)	
			Uniform	Total	Yield	Ultimate
CA-0218-A-5	None	27	8.64	16.7	26,500	32,100
-6	None	200	3.15	17.9	18,520	19,580
-7	None	300	2.66	18.7	13,200	14,600
-10	None	400	1.53	37.1	7,640	8,200
-8	None	450	2.12	41.5	5,300	5,710
CA-0218-2-5	2	27	7.63	12.1	26,180	33,800
-3	2	200	2.29	6.51	19,470	21,035
-2	2	300	1.33	7.55	14,790	16,190
-4	2	400	0.96	14.8	10,190	10,440
-1	2	450	1.45	7.05	7,640	8,140
CA-0218-8-6	8	27	3.40	4.82	53,700	61,500
-4	8	200	1.16	2.67	41,700	43,050
-3	8	300	1.09	1.34	29,200	31,500
-7	8	400	1.09	1.31	21,400	22,560
-8	8	450	1.43	1.71	17,800	19,000
CA-0218-10-8	10	27	1.53	1.53	49,400	53,300
-5	10	200	1.29	3.43	36,700	38,547
-6	10	300	0.88	2.21	27,700	29,500
-4	10	400	0.56	0.93	21,900	22,290
-7	10	450	0.66	1.05	18,000	18,200
CA-0218-12-7	12	27	5.40	7.44	42,100	48,800
-3	12	200	1.14	2.52	35,390	36,810
-4	12	300	0.91	3.15	26,100	27,100
-9	12	400	0.90	2.75	18,220	19,020
-8	12	450	1.19	2.40	15,200	15,900

[a]Made from aluminum powder alloyed with 2.1% Mo, 0.07% Fe, 2.4% Zr, 0.13% Ti, 0.076% V, and 0.25% Cr.

TABLE 18

TENSILE PROPERTIES OF DISPERSION STRENGTHENED ALLOY CA-0219[a]

Sample No.	Ball-Milling Time (hr)	Test Temperature (°C)	Elongation (%)		Tensile Strength (psi)	
			Uniform	Total	Yield	Ultimate
CA-0219-A-10	None	27	8.63	18.4	20,500	25,100
-9	None	200	3.55	12.7	14,570	15,760
-7	None	300	1.84	17.4	10,900	11,600
-8	None	450	2.16	52.0	4,970	5,220
CA-0219-2-5	2	27	6.29	9.14	26,350	33,310
-3	2	200	2.36	8.05	20,460	21,290
-2	2	300	1.04	2.70	15,200	15,980
-4	2	400	0.82	3.20	11,520	11,930
-1	2	450	1.09	3.13	9,110	9,610
CA-0219-8-6	8	27	4.86	6.15	43,400	52,000
-10	8	200	1.97	2.99	34,480	38,220
-11	8	300	1.34	3.05	27,800	30,100
-7	8	400	0.64	1.62	23,270	23,760
-9	8	450	0.69	1.05	19,900	20,500
CA-0219-12-5	12	27	3.31	4.29	47,500	53,300
-9	12	200	1.22	1.89	37,190	39,450
-7	12	300	1.37	4.82	27,500	29,300
-8	12	400	1.03	3.24	20,210	20,780
-10	12	450	2.24	3.06	15,100	16,600

[a]Made from aluminum powder alloyed with 3.8% Mo, 0.09% Fe, 0.7% Zr, 0.034% Ti, 0.058% V, and 0.056% Cr.

TABLE 19

TENSILE PROPERTIES OF DISPERSION STRENGTHENED ALLOY CA-0222[a]

Sample No.	Ball-Milling Time (hr)	Test Temperature (°C)	Elongation (%)		Tensile Strength (psi)	
			Uniform	Total	Yield	Ultimate
CA-0222-A-9	None	27	8.11	19.2	23,400	30,200
-8	None	200	2.34	16.1	18,590	20,370
-10	None	300	1.77	17.3	14,100	15,100
-6	None	400	2.07	22.0	9,220	9,701
-7	None	450	3.44	31.0	7,190	8,200
CA-0222-2-5	2	27	5.98	9.18	23,510	30,650
-2	2	300	1.31	14.5	14,050	14,610
-4	2	300	0.69	8.15	10,190	10,350
-1	2	450	0.49	6.00	8,280	8,400
CA-0222-8-4	8	27	0.70	0.70	55,400	59,000
-6	8	200	1.12	2.81	44,540	46,390
-9	8	300	1.25	1.46	31,000	32,900
-5	8	400	0.98	3.08	20,940	21,670
-7	8	450	2.26	2.47	15,200	16,800
CA-0222-10-6	10	27	3.44	3.44	48,600	55,800
-5	10	200	1.26	2.06	40,420	42,040
-7	10	450	0.66	1.02	20,800	21,300
CA-0222-12-7	12	27	1.64	1.64	55,400	60,300
-9	12	200	1.09	2.07	42,540	44,940
-4	12	300	0.91	1.69	30,300	32,100
-6	12	400	0.60	0.87	22,390	23,040
-8	12	450	0.59	0.66	18,700	19,600

[a]Made from aluminum powder alloyed with 4.4% Mo, 1.7% Fe, 1.4% Zr, 0.064% Ti, 0.037% V, and 0.83% Cr.

TABLE 20

TENSILE PROPERTIES OF DISPERSION STRENGTHENED ALLOY CA-0223[a]

Sample No.	Ball-Milling Time (hr)	Test Temperature (°C)	Elongation (%)		Tensile Strength (psi)	
			Uniform	Total	Yield	Ultimate
CA-0223-A-9	None	27	7.84	15.6	30,000	37,000
-5	None	200	3.10	13.7	25,440	26,430
-8	None	300	3.16	14.3	16,800	18,600
-6	None	400	2.34	24.0	11,160	11,880
-7	None	450	3.98	31.0	6,080	6,850
CA-0223-2-5	2	27	5.98	10.4	30,880	37,750
-3	2	200	5.01	10.1	23,200	26,190
-2	2	300	1.82	8.57	17,340	18,620
-4	2	400	0.81	8.82	12,070	12,420
-1	2	450	1.04	7.72	9,220	9,540
CA-0223-8-10	8	27	2.87	2.87	52,700.	63,500
-7	8	200	1.89	2.25	44,140	47,510
-6	8	300	1.14	2.17	33,000	35,400
-9	8	400	0.64	1.74	25,440	26,160
-8	8	450	1.02	1.50	19,700	21,200
CA-0223-10-8	10	27	3.13	4.02	43,200	47,900
-4	10	200	1.22	5.67	32,740	34,760
-5	10	300	1.22	6.84	24,500	25,700
-9	10	400	1.15	3.99	16,570	17,380
-7	10	450	1.27	2.69	14,300	14,900

[a]Made from aluminum powder alloyed with 4.1% Mo, 4.1% Fe, 0.25% Zr, 0.12% Ti, 0.02% V, and 0.33% Cr.

TABLE 21

TENSILE PROPERTIES OF DISPERSION STRENGTHENED ALLOY CA-0224[a]

Sample No.	Ball-Milling Time (hr)	Test Temperature (°C)	Elongation (%)		Tensile Strength (psi)	
			Uniform	Total	Yield	Ultimate
CA-0224-A-5	None	27	7.66	13.6	27,200	34,900
-6	None	200	4.08	11.6	21,720	24,250
-7	None	300	2.07	17.1	15,700	16,900
-9	None	400	1.68	18.5	9,950	10,510
-8	None	450	4.95	37.6	6,870	7,700
CA-0224-2-5	2	27	5.75	8.42	30,910	38,910
-3	2	200	3.23	6.52	23,330	25,610
-2	2	300	0.87	6.65	18,030	18,600
-4	2	400	1.31	4.69	11,260	12,490
-1	2	450	1.00	4.29	10,270	10,560

[a]Made from aluminum powder alloyed with 4.9% Mo, 1.7% Fe, 0.24% Zr, 0.09% Ti, 0.046% V, and 0.054% Cr.

VITA

George Larry Copeland was born in Gadsden, Alabama, on July 3, 1941. He attended local schools and was graduated from Etowah County High School in 1959. In January, 1963, he received a Bachelor of Science degree in Metallurgical Engineering from the University of Alabama. From then until August, 1965, he was employed by the General Electric Company at Knolls Atomic Power Laboratory. In June, 1965, he received a Master of Science degree with a major in Metallurgical Engineering from Rensselaer Polytechnic Institute.

Since September, 1965, he has been employed by the Union Carbide Corporation, Nuclear Division, at two of their Oak Ridge facilities. He was at the Oak Ridge National Laboratory until 1973, and is currently at the Oak Ridge Gaseous Diffusion Plant. In 1965, he entered the Graduate School at the University of Tennessee and received the Doctor of Philosophy degree with a major in Metallurgical Engineering in March, 1975.

He is married to the former Betty Jane Fortenberry of Gasden, Alabama. They have two children.